Quaternary Science Reviews 234 (2020) 106207

Contents lists available at ScienceDirect

Quaternary Science Reviews

journal homepage: www.elsevier.com/locate/quascirev

A complete Holocene lake sediment ancient DNA record reveals long-standing high Arctic plant diversity hotspot in northern Svalbard

Linn H. Voldstad [a, b, *], Inger G. Alsos [c], Wesley R. Farnsworth [a, d, e], Peter D. Heintzman [c], Lena Håkansson [a], Sofia E. Kjellman [d], Alexandra Rouillard [d, f], Anders Schomacker [d], Pernille B. Eidesen [a]

[a] The University Centre in Svalbard (UNIS), P.O. Box 156, N-9171, Longyearbyen, Norway
[b] Faculty of Environmental Sciences and Natural Resource Management, Norwegian University of Life Sciences, P.O. Box 5003 NMBU, N-1432 Ås, Norway
[c] The Arctic University Museum of Norway, UiT The Arctic University of Norway, P.O. Box 6050, Langnes, N-9037, Tromsø, Norway
[d] Department of Geosciences, UiT The Arctic University of Norway, P.O. Box 6050, Langnes, N-9037, Tromsø, Norway
[e] NordVulk, Nordic Volcanological Center, Institute of Earth Sciences, University of Iceland, Askja, Sturlugata 7, IS-101 Reykjavik, Iceland
[f] Centre for GeoGenetics, University of Copenhagen, Øster Voldgade 5-7, DK-1350, Copenhagen K., Denmark

ARTICLE INFO

Article history:
Received 11 December 2019
Received in revised form
1 February 2020
Accepted 2 February 2020
Available online 9 March 2020

Keywords:
Ancient DNA
SedaDNA
Holocene
Lake sediments
Metabarcoding
Svalbard
Vegetation dynamics
Biodiversity hotspot

ABSTRACT

Arctic hotspots, local areas of high biodiversity, are potential key sites for conservation of Arctic biodiversity. However, there is a need for improved understanding of their long-term resilience. The Arctic hotspot of Ringhorndalen has the highest registered diversity of vascular plants in the Svalbard archipelago, including several remarkable and isolated plant populations located far north of their normal distribution range. Here we analyze a lake sediment core from Ringhorndalen for sedimentary ancient DNA (*sed*aDNA) and geochemical proxies to detect changes in local vegetation and climate. Half of the plant taxa appeared already before 10,600 cal. yr BP, indicating rapid colonization as the ice retreated. Thermophilous species had a reoccurring presence throughout the Holocene record, but stronger signal in the early than Late Holocene period. Thus, thermophilous Arctic plant species had broader distribution ranges during the Early Holocene thermal maximum *c.* 10,000 cal. yr BP than today. Most of these thermophilous species are currently not recorded in the catchment area of the studied lake, but occur locally in favourable areas further into the valley. For example, *Empetrum nigrum* was found in >40% of the *sed*aDNA samples, whereas its current distribution in Ringhorndalen is highly restricted and outside the catchment area of the lake. Our findings support the hypothesis of isolated relict populations in Ringhorndalen. The findings are also consistent with main Holocene climatic shifts in Svalbard identified by previous studies and indicate an early warm and species-rich postglacial period until *c.* 6500 cal. yr BP, followed by fluctuating cool and warm periods throughout the later Holocene.

1. Introduction

Biodiversity hotspots are localities of high species diversity. Such localities have been suggested as crucial sites for the long-term persistence of species and are thus key sites for conservation, especially in a changing climate (Myers et al., 2000; Elvebakk, 2005; CAFF, 2013). However, long-term observations of persistence are lacking. To fill this knowledge-gap, paleoecological records can provide insight into past vegetation and species persistence valuable for conservation (Willis et al., 2007) alongside the reconstruction of past climates (e.g. Birks et al., 1994; Berglund et al., 1996; Alsos et al., 2016; Clarke et al., 2019b).

Traditional paleobotanical proxies can be challenging in the Arctic due to low production of local pollen and plant macrofossils (Lamb and Edwards, 1988; Vasil'chuk 2005; Birks, 1991). In contrast, the cold conditions favor DNA preservation of what little may be produced (Hofreiter et al., 2001). Next generation sequencing methods have drastically increased the potential for DNA-based investigations in paleoecological studies over the past decade (Taberlet et al., 2007; Parducci et al., 2017), and the metabarcoding of *sed*aDNA has proven an efficient tool for

* Corresponding author. Department of Biological Science, University of Bergen, Thormøhlensgt. 53a, N-5006, Bergen, Norway.
E-mail address: linnmhv@gmail.com (L.H. Voldstad).

https://doi.org/10.1016/j.quascirev.2020.106207

reconstructing past vegetation and species diversity (Sønstebø et al., 2010; Willerslev et al., 2014; Zimmermann et al., 2017a).

Lake basins trap detrital and organic material from both the catchment and in-lake production. Lake sediment records are therefore excellent archives for inferring regional climate (Gjerde et al., 2017). Sedimentological, magnetic, geochemical and physical sediment properties can be used as proxies to reconstruct major patterns in abiotic environmental changes in the catchment. High-resolution elemental composition can be obtained from X-ray fluorescence (XRF) scans. Combined with the profiles of magnetic susceptibility (MS) and lithogenic, geochemically-stable, and conservative elements, these indicators can infer climate variability. Silica (Si), titanium (Ti), potassium (K), iron (Fe) and calcium (Ca) can, for instance, reflect changes in glacially-derived minerogenic input (Sandgren and Snowball, 2001; Schomacker et al., 2019), grain size (Cuven et al., 2010), weathering regimes (Rothwell and Croudace, 2015), the amount of inorganic detrital input to a lake (Røthe et al., 2015) and biological lake-production (Balascio et al., 2011; Kylander et al., 2011; Melles et al., 2012; Alsos et al., 2016; Gjerde et al., 2017; de Wet et al., 2018).

The majority of paleoecological and geological records indicates that the Early-Mid Holocene period in Svalbard was warmer than today (*c.* 9000-5000 years ago; Hyvärinen, 1970; Birks, 1991; Birks et al., 1994; Salvigsen and Høgvard, 2006; Miller et al., 2010; Alsos et al., 2016; Farnsworth, 2018). According to Mangerud and Svendsen (2018), the August sea-surface temperature was possibly as much as 6 °C higher than today. Based on present-day distributions, clone sizes, and genetic patterns, it is assumed that the most thermophilous plants in Svalbard had a broader distribution during the Early Holocene (Alsos et al., 2002; Engelskjøn et al., 2003; Birkeland et al., 2017). For some species, this has been confirmed by *sed*aDNA and/or plant macrofossil records from several lakes in the Svalbard archipelago (Birks, 1991; Wohlfarth et al., 1995; Alsos et al., 2016).

Ringhorndalen and the neighbouring valley Flatøyrdalen (Fig. 1) are the most botanically diverse locations in Svalbard, and assumed to have remnants from the Early Holocene vegetation (Elvebakk and Nilsen, 2002, 2016; Eidesen et al., 2013; Birkeland et al., 2017). Flatøyrdalen has been described as an 'Arctic hotspot' due to its "extrazonally warm climate, resulting in thermophilous

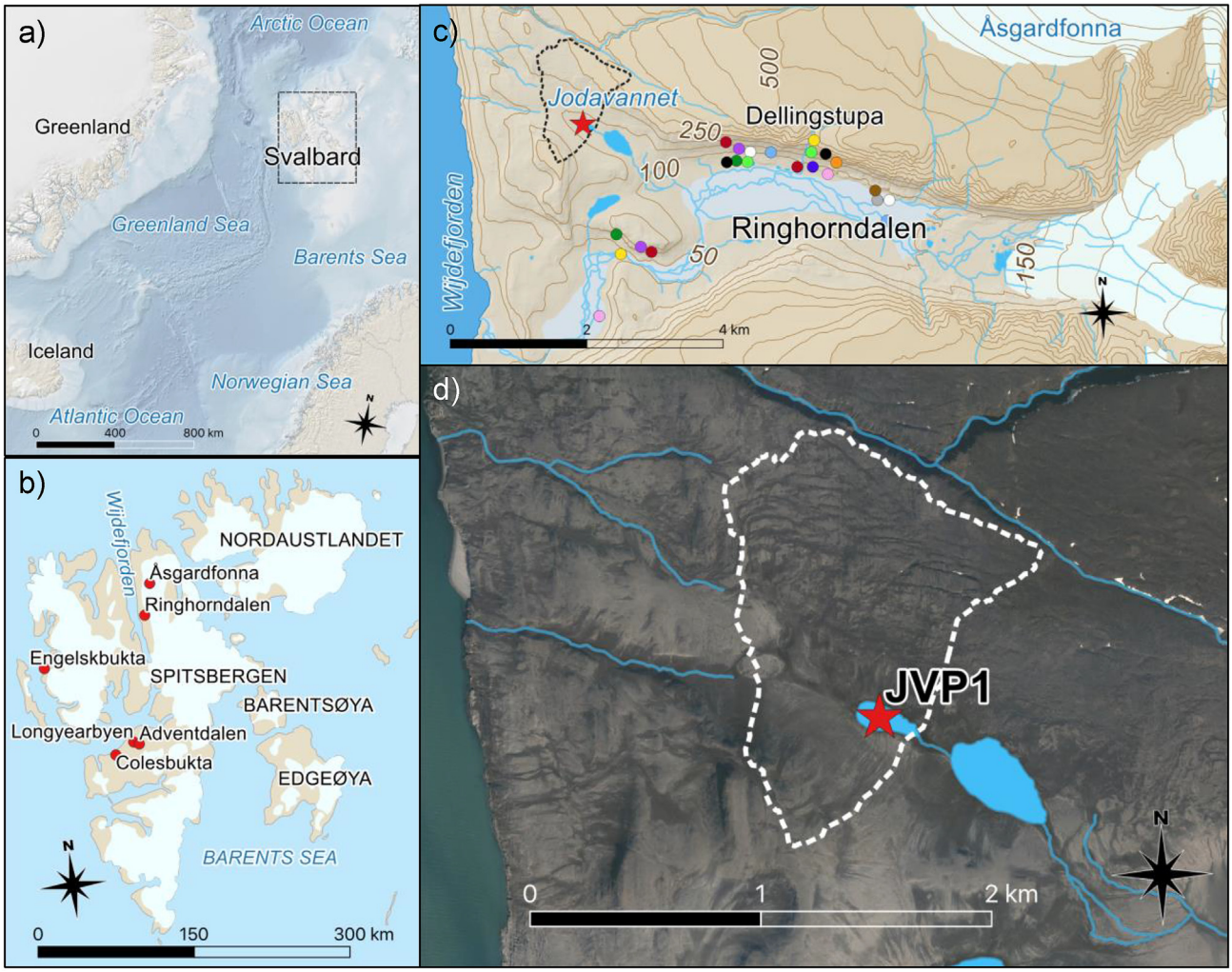

Fig. 1. (a) The North Atlantic Ocean with the location of (b) the Svalbard archipelago and (c-d) the study site in Ringhorndalen. Hatched lines around Jodavannet mark the catchment and the red star marks sampling location of the sediment core used for all analyses. Coloured circles in (c) indicate current local distributions of thermophilous vascular plant species (https://artskart.artsdatabanken.no, 2019): *Arenaria humifusa* (grey), *Arnica angustifolia* (yellow), *Calamagrostis purpurascens* (dark red), *Carex bigelowii* ssp. *arctisibirica* (brown), *Carex krausei* (dark green), *Carex saxatilis* ssp. *laxa* (pink), *Campanula uniflora* (dark blue), *Comastoma tenellum* (light blue), *Empetrum nigrum* ssp. *hermaphroditum* (purple), *Luzula spicata* (orange), *Pinguicula alpina* (white), *Tofieldia pusilla* (light green) and *Vaccinium uliginosum* ssp. *microphyllum* (black). Maps modified from The Norwegian Mapping Authority and The Norwegian Polar Institute.

biodiversity elements not found in its surroundings" (Elvebakk, 2005). Many of the unusually thermophilous plant species occurring in the area are spatially distant from their normal distribution range. Of the 124 vascular plant species known from the area, some populations represent the northernmost known sites for the species worldwide and the only known location in Svalbard (*Pinguicula alpina*, *Luzula spicata*, *Erigeron uniflorus, Draba* aff. *oblongata* and *Festuca ovina*) or Europe (*Calamagrostis purpurascens*) (Elvebakk and Nilsen, 2002, 2016; Eidesen et al., 2013, 2018).

In this study, we investigate sediments from a lake in Ringhorndalen using metabarcoding of *sed*aDNA, sedimentology, and geochemical proxy data to reconstruct changes in vegetation composition and postglacial environmental conditions. We aim to answer the following questions: (i) How has the composition of plants in the catchment area developed since the last deglaciation? (ii) Can *sed*aDNA together with elemental data increase our understanding of Holocene climate variability?

2. Setting

Ringhorndalen is situated at the east coast of Wijdefjorden on northern Spitsbergen (Fig. 1). The sediment core was obtained from lake Jodavannet (informal name; 79.3383 °N, 16.0167 °E; Fig. 1d), which is situated 140 m a.s.l. on the northern side of the valley mouth.

2.1. Local climate and modern growth conditions

No meteorological data record exist for the area, but the current climate can partly be inferred from local vegetation and the glacier equilibrium line altitude (ELA). Elvebakk and Nilsen (2002) concluded that the vegetation in the outer areas of Ringhorndalen reflects relatively high temperatures combined with aridity due to low precipitation and wind desiccation. ELAs of >800 m a.s.l. on the glaciers in the inner part of Wijdefjorden indicate low precipitation in the region (Hagen et al., 1993). Based on observations of snowlines and mass balance of selected glaciers, Hagen et al. (1993) inferred a mean annual precipitation of 200 mm in the inner Wijdefjorden area, including Ringhorndalen.

Eidesen et al. (2018) measured climatic (temperature, moisture, radiation) and soil abiotic variables (pH, organic content via loss-on-ignition (LOI) and carbon-to-nitrogen (C:N) ratio) during one growing season from May to July 2017. The results revealed warmer growth conditions in Ringhorndalen compared to reference sites in Adventdalen (e.g. mean July soil temperature in *Dryas* heath in Ringhorndalen was 9.4 ± 1.4 °C, whereas it was 6.8 ± 0.5 °C in Adventdalen, based on four loggers at each location). Light and moisture measurements showed few cloudy days and the main moisture to be input from snowmelt early in the season rather than summer precipitation. The recorded soil pH was close to neutral (mean = 6.7, range = 5.1–7.9), with the highest values in the valley mouth. The organic C content in soil from zonal vegetation was within the expected range for bioclimatic zone C (10–30%) according to Jónsdóttir (2005). The N content was variable between samples (0.39 ± 0.27% (±SD)), but in line with measurements in other productive areas of Svalbard such as Colesbukta and Engelskbukta on the west coast (P.B. Eidesen, unpublished data; Fig. 1b). The C:N ratio of 13.01 ± 2.71 (mean ± SD) indicates good decomposition conditions according to Eidesen et al. (2018).

2.2. Geology, topography and vegetation

The bedrock in the catchment of Jodavannet consists of Mesoproterozoic micaschist, metapsammite and amphibolite. Further upvalley the bedrock consists of Palaeoproterozoic granitic gneiss, migmatite and amphibolite. The easternmost part of Ringhorndalen consists of Mesoproterozoic quartzite, micaschist, amphibolite and marble (Dallmann, 2015). The valley floor is mostly occupied by outwash, with braided meltwater rivers that originate from two confluent outlet glaciers from the Åsgardfonna ice cap in the inner part of the valley (Fig. 1c). Situated at 140 m a.s.l., Jodavannet is above the regional postglacial marine limit of *c.* 65 m a.s.l. (Forman et al., 2004). It has an area of 0.02 km^2. At present, the catchment of Jodavannet (1.31 km^2; Fig. 1c–d) has no glacial meltwater input as it is separated from the rivers draining the glaciers by topographic boundaries. Runoff is brought to the lake from the northern, western, and southern slopes. A small stream enters from northwest, and the lake drains into a larger lake in southeast (Fig. 1d). Traces of erosion from water flow towards the lake can be seen on the southern and southwestern sides (Fig. 1d).

The valley mouth has distinct high-Arctic steppe vegetation with prevalent *Potentilla pulchella* communities (Elvebakk and Nilsen, 2002). This is where the wind tunnel effect from Wijdefjorden is strongest. Small ridges separate the outer valley where Jodavannet is located from the more wind-sheltered and thus warmer inner valley, where most of the thermophilous plant species are growing today. The catchment therefore includes only some of the most thermophilous flora elements. Upslope on the steep valley sides, particularly lush gullies, open screes, and sheltered boulder fields stretch down from vertical headwalls higher up. *Cassiope tetragona* heath dominates further downslope.

At present, the vegetation around Jodavannet is homogenous, with a moss-dominated belt stretching up to 5 m from the lake shore. *Saxifraga oppositifolia*, *Carex subspathaceae*, *Dupontia fisheri*, *Bistorta vivipara* and *Salix polaris* are the most frequent vascular plant species in the closest 30 m around the lake (Table C, Appendix A). In general, there are mainly temperature-indifferent species (*sensu* Elvebakk, 1989), but some weakly thermophilous species are also common within close proximity to the lake, e.g. *Carex subspathacea, Equisetum arvense* ssp. *alpestre*, and *Cardamine pratensis*, while *Dryas octopetala* (weakly thermophilous) and *Cassiope tetragona* (distinctly thermophilous) have occurrences further away.

3. Methods

3.1. Sediment coring and subsampling

A 186 cm long sediment core (JVP1) was taken from the deepest part of the lake (79.33831 °N; 16.01902 °E) at a water depth of 6.4 m, in August 2016. Coring was performed with a hand-held lightweight piston corer equipped with 60 mm diameter and 200 cm long coring tubes. The core was kept sealed and refrigerated during transfer to the Centre for GeoGenetics, University of Copenhagen, Denmark, where *c.* 2–5 g subsamples were taken along the entire core length at 2 cm intervals, following the clean sampling procedures described by Pedersen et al. (2016). The subsamples were kept cold and transported to Tromsø Museum, at UiT The Arctic University of Norway, where they were stored frozen (−18 °C) until further processing.

3.2. Age-depth modelling

To establish a chronology for JVP1, nine terrestrial and aquatic macrofossils were retrieved from the core by wet sieving of *c.* 10 cm^3 of sediment. All macrofossils were radiocarbon (^{14}C) dated with accelerator mass spectrometry (AMS) at the Tandem Laboratory at Uppsala University, Sweden, and the Radiocarbon Dating Laboratory at Lund University, Sweden (Table 1).

Using the nine ^{14}C ages, an age-depth model was constructed

Table 1
Radiocarbon dates for the sediment core from *Jodavannet* shown with 1σ error, calibrated median ages (individual samples were calibrated with *OxCal 4.3* and modelled with *Bacon 2.2*), calibrated 95% confidence age ranges, sample material and sample weight.

Depth (cm)	Lab number	^{14}C age (yr BP)	Sample median age (cal. yr BP)	Modelled median age (cal. yr BP)	Modelled 2σ age range (cal. yr BP)	Sample material	Sample weight (mg)
12.0–13.0	Ua-55361	279 ± 24	370	306	431–0	*Salix polaris*	4.3
37.0–38.0	Ua-55362	767 ± 26	693	703	902–655	*Salix polaris*	2.2
52.0–53.0	Ua-55363	1977 ± 25	1925	1900	2015–1803	*Salix polaris*	1.3
65.0–66.0	LuS-14000	3010 ± 40	3200	3134	3353–2958	Aquatic bryophyte	1.3
80.0–81.0	LuS-14001	3945 ± 40	4396	4288	4506–4061	Aquatic bryophyte	0.7
128.5–129.5	Ua-55364	4968 ± 34	5691	5730	5943–5506	*Salix polaris**	0.7
144.0–145.0	LuS-14002	8335 ± 45	9358	9149	9513–8584	Aquatic bryophyte	1.2
177.0–178.0	Ua-55365	9512 ± 40	10814	10922	11167–10528	*Salix polaris**	0.9
185.0–186.0	Ua-55366	10426 ± 42	12302	11870	12215–11585	Aquatic bryophyte	2.9

Macrofossils were ^{14}C dated at Uppsala University (Ua-) and Lund University (LuS-). Radiocarbon ages of macrofossils were calibrated following IntCal13 (Reimer et al., 2013) using the software Bacon 2.2 (Blaauw and Christen, 2011) with default settings. Samples were taken over 1 cm intervals, thus calibrated ages are given for the intermediate value (±0.5) from the model output. *Some small stems from other vascular plants than *Salix polaris* were included to provide enough dateable material.

with the Bayesian software 'Bacon' (v. 2.2; Blaauw and Christen, 2011) within 'R' (v.3.4.3; R Core Team, 2017). The model run had default prior settings, resulting in a mean sedimentation time (acc. mean) of 50 years/cm. Resulting ages are reported in calibrated radiocarbon years before present (cal. yr BP; BP = AD 1950) according to the calibration curve IntCal13 (Reimer et al., 2013). The program divided the cores into many vertical sections of equal thickness and estimated sedimentation rates (years/cm) through millions of Markov Chain Monte Carlo (MCMC) iterations. Ages were calculated for every 0.5 cm of JVP1 within pre-defined range limits (8–185.5 cm). To estimate ages for all *sed*aDNA samples, the calibrated age estimates were extrapolated above the youngest ^{14}C age at 12 cm depth. The calibrated age for the uppermost sample (from 8 cm depth) must consequently be treated with caution.

3.3. Lithological analyses

High-resolution optical (90 μm) and X-ray imagery (200 μm), XRF (1000 μm), and MS (4000 μm) were obtained from Itrax scanning, performed at the Centre for GeoGenetics, University of Copenhagen (Itrax CS37 Cph; Croudace et al., 2006). Scans were carried out using a rhodium (Rh) tube with voltage and current set to 30 kV and 50 mA, respectively, and the XRF count time was 35 s. Variations in MS (Thompson et al., 1975) and elemental profiles in kilo counts per second (kcps) from XRF scanning (Kylander et al., 2011; Löwemark et al., 2011) were used as proxies for variations in environmental conditions in the catchment area of the lake (Rothwell and Rack, 2006; Rothwell et al., 2006). Additionally, percentage organic content of the sediments was measured by LOI (Heiri et al., 2001). Samples of 2 cm^3 were sampled at 1 cm intervals throughout the core, dried at 105 °C for 24 h and ignited at 550 °C for 4 h. The profiles of LOI, MS and 6 different elements/elemental ratios are used to describe long-term environmental variation reflected in the geochemistry of the sediment record. To reduce noise, the MS and elemental values were modified with a weighted moving average (*pracma* package; 5-points backward window length), resulting in measurement intervals of 1.6 cm (MS) and 0.5 cm (elemental values; Gjerde et al., 2017), and the conservative element Ti was used to normalize the element profiles. Ti was normalized against the sum of the coherent (coh) and incoherent (inc) scatter from rhodium (Rh).

High MS signal in lake sediments can reflect inorganic allochthonous material (Thompson et al., 1975) and was used as proxy for minerogenic input (Snowball and Sandgren, 1996; Schomacker et al., 2019). Rh coh versus Rh inc was used as a density proxy, typically reflecting dense sediments of minerogenic origin.

Typical allogenic elements such as Ti, Ca and K have previously been used to reflect erosion intensity. High Ti values can indicate increased detrital sediment input from glacial or aeolian deposition as well as erosion and runoff from the catchment (Rothwell and Croudace, 2015; Davies et al., 2015). High K/Ti values were evaluated as potential increased weathering, because K is relatively water-soluble compared to the more stable Ti (Rothwell and Croudace, 2015). To assess changes in biological production, Ca/Ti and Si/Ti were used to indicate biogenic silica production in the lake (Melles et al., 2012; Liu et al., 2013).

3.4. SedaDNA extraction, metabarcoding, and high throughput sequencing

*Sed*aDNA was extracted from entire subsamples (2–5 g; n = 41) and negative extraction controls (n = 6) in the ancient DNA dedicated laboratory at Tromsø Museum. We extracted a greater proportion of subsamples from the deeper layers of JVP1 to increase resolution in the earliest time-period (8–101 cm, n = 10; 110–135 cm, n = 7; 138–185 cm, n = 24). A modified DNeasy PowerMax Soil DNA Isolation kit protocol (Qiagen Norge, Oslo, Norway) was used for extraction. In addition to the cell disruptive solution ("C1"), 100 μL of 5 mg/mL proteinase K and 400 μL of 1M dithiothreitol (DTT) were added to each sample. The subsequent vortexing of samples was conducted in a FastPrep-24 TM 5G (M. P. Biomedicals LLC, Santa Ana, CA, USA) for 2 × 20 s at 4.5 m/s and then incubated at 56 °C for *c.* 15 h (following Alsos et al., 2016; Zimmermann et al., 2017b). All centrifuge steps were conducted at 4200 rpm instead of 2500 rpm. In the final step, all samples were recovered in 3 mL instead of 5 mL elution buffer (Alsos et al., 2016).

For metabarcoding, all polymerase chain reactions (PCRs) were setup in the dedicated ancient DNA laboratory at Tromsø Museum, which is physically isolated from other PCR work to prevent contamination from PCR products. Two negative PCR controls (one from the aDNA lab and one from the PCR lab) and one positive control with synthetically reconstructed sequence were amplified in addition to the 41 DNA extracts from samples and six negative extraction controls, thus in total 50 samples/controls. The target region was the short P6-loop of the chloroplast *trn*L (UAA) intron, amplified with the universal plant primers *g* and *h* (Taberlet et al., 2007). These primers amplify vascular plant taxa, but may also sporadically detect other non-vascular plants (Taberlet et al., 2018). Unique flanking sequences (*tags*) 8 or 9 base pairs (bp) long were added at the 5' end to allow for PCR product pooling. Seven PCR replicates were conducted per sample and control to increase the chance of detecting rare taxa and taxa with low template DNA representation in the sediment record, and to facilitate distinguishing probable true from false positives (Ficetola et al., 2015;

Alsos et al., 2018a). DNA amplification was conducted in 40 μL final volumes, containing 4 μL of undiluted DNA extract, 1X Gold buffer, 1.6 U of AmpliTaq Gold ® DNA Polymerase (Life Technologies, Carlsbad, CA, USA), 2.5 mM $MgCl_2$, 0.2 mM dNTPs, 0.2 μM forward primer, 0.2 μM reverse primer, and 160 ng/μL Bovine Serum Albumin. The PCR mixtures underwent enzyme activation for 10 min at 95 °C, followed by 45 cycles of denaturation for 30 s at 95 °C, annealing for 30 s at 50 °C, and elongation for 1 min at 72 °C, plus a final elongation step for 7 min at 72 °C.

10 μL from each PCR product was pooled and the resulting mix purified using the Qiagen MinElute PCR purification kit (Qiagen GmbH, Hilden, Germany), following the manufacturer's instructions (Alsos et al., 2016). The purified amplicon pool was sent to FASTERIS (FASTERIS SA, Switzerland), where it was converted into an Illumina-compatible DNA library using the single-indexed, PCR-free MetaFast protocol. The library was sequenced on an Illumina NextSeq 500 sequencing platform (Illumina, Inc., CA, USA) using 10% of a mid-output, 2 × 150 cycle flow cell.

3.5. Bioinformatic analyses and taxonomical assignment

The OBITools software package (Boyer et al., 2016) was used to analyze sequence data, and the analysis was run through the Abel computing cluster at University of Oslo. Amplicons were reconstructed by aligning paired-end reads with *illuminapairedend*, and sequences having an alignment score lower than 40 (Alsos et al., 2016) were removed with *obigrep*. The remaining sequences were assigned to samples according to their unique sample tags with *ngsfilter* (demultiplexing), requiring 100% match with tags and maximum 2 bp mismatch in the primer region (default options in OBITools). As *ngsfilter* does not allow different tag lengths, this step was run twice and resulted in two output files that were subsequently merged with the UNIX *cat* command. Amplicons with unexpected tag combinations were considered chimerical sequences and thus removed with *obigrep*. To exclude sequences shorter than those in the reference library, *obigrep* was also used to remove sequences shorter than 10 bp.

Identical sequences were clustered (deduplication) using *obiuniq*, keeping the information about their distribution among samples. Sequences with only one copy in the dataset were removed (Alsos et al., 2016) with *obigrep*, before using *obiclean* to identify sequences potentially resulting from PCR and sequencing errors. Using information about sequence record counts and sequence similarities across all samples, sequences were classified as *head* (ideally true sequences), *singleton* (potentially rare true sequences) or *internal* (assumed erroneous sequences; Boyer et al., 2016). A maximum of a single base-pair difference was allowed between two variant sequences, and the abundance threshold ratio for the uncommon *internal* versus common *head* sequence was 5%. This threshold retained relatively rare sequences, as small sequence differences may make a taxonomically important difference to P6-loop sequence identification (Sønstebø et al., 2010; Alsos et al., 2016). Sequences with no close resemblance to others (neither *head* nor *internal*), were classified as *singleton*. To avoid potential PCR or sequencing errors, only *head* and *singleton* sequences were kept.

Finally, sequences were assigned to taxa based on sequence similarity with two taxonomic reference libraries, using *ecotag* (part of the OBITools package). The primary reference library (*arctborbryo*) contains local taxa of 815 Arctic (Sønstebø et al., 2010) and 835 boreal (Willerslev et al., 2014) vascular taxa in addition to 455 bryophytes (Soininen et al., 2015), which covers the majority of plant species growing in Svalbard at present (Alsos et al., 2018b). The secondary reference library contains sequences from running *ecopcr* on the global EMBL Nucleotide Sequence Database (R134, January 2018). The EMBL reference library was used to detect possible non-local contaminants. This resulted in two files containing the unique sequences and their taxonomic assignment from each reference library.

After initial data processing with OBITools, further filtering of the sequences was conducted in R. To avoid misidentifications, only sequences with a 100% match to reference library sequences were kept. Next, the two result files were merged, keeping only the *arctborbryo*-assigned sequence in the case of conflicts. To minimize the chance of including false positives, we registered sequences as present in a sample if the sequence: 1) had a minimum of 10 reads per PCR replicate and occurred in a minimum of two PCR replicates, 2) was not detected in the negative controls, and 3) occurred in a minimum of 100 reads across the entire dataset. Sequences matching non-native or marine taxa were compared to the NCBI nucleotide database using BLAST (http://www.ncbi.nlm.nih.gov/blast/; Accessed April 2018) to confirm if they were correctly assigned to unlikely taxa in the study area. Some sequences were assigned with low taxonomic resolution from their taxon ID in the NCBI taxonomy database. These sequences were also compared to the NCBI nucleotide database to improve taxonomic assignment. Consequently, some taxonomic names were modified according to the BLAST-results and accepted taxonomy in the local botanical literature (Elven et al., 2011) (*Carex* sp. changed to *Carex saxatilis*, *Cassiope lycopodioides* to *Cassiope tetragona*, *Pedicularis* sp. to *Pedicularis dasyantha*/*hirsuta*, *Festuca pratensis* to *Festuca* sp. (5 species), *Ranunculus sceleratus* to *Ranunculus hyperboreus*, Polypodiales to *Cystopteris fragilis* and *Nannochloropsis granulata* to *Nannochloropsis* sp.; Table 2). The resulting taxonomy after modifications was used in all subsequent analyses. Two exotic taxa (*Cedrus* and *Juniperus*) were suspected contaminants and therefore removed from the dataset.

3.6. Constrained hierarchical cluster analysis

All statistical analyses were conducted in R. To categorize the Holocene development of species communities as found by metabarcoding, the *vegdist* function in R-package *vegan* (Oksanen et al., 2017) was used to create a matrix of Bray-Curtis dissimilarity indices of all identified unique taxa based on number of PCR replicates per sample. Sequences that were undifferentiated between several different species or identified to taxonomic levels precluding ecological interpretation, were merged before subsequent analysis (*Festuca* sp. and *Festuca baffinensis/brachyphylla/edlundiae/hyperborea/ovina/rubra*; five sequences of *Saxifraga* sp.; four sequences of 'Hypnales'; *Ranunculus hyperboreus/gmelinii* and two sequences of *Ranunculus sceleratus*; and two sequences of *Pedicularis hirsuta/dasyantha*). The dissimilarity matrix was then clustered with the *chclust* function from *vegan*, using constrained hierarchical clustering with clusters constrained by sample depth and the *coniss* algorithm (Grimm, 1987). To identify the number of statistically significant groups from the constrained cluster analysis, a broken stick distribution (Bennett, 1996) was created with the *bstick* function from the *rioja* package (Juggins, 2017).

4. Results

4.1. Chronology

The age-depth model returned a median age range of 11,870-306 cal. yr BP (Table 1; Fig. 2). Age-depth model convergence was indicated by the relatively stationary and unstructured adjacent MCMC iterations (Fig. A, Appendix A).

Table 2
All taxa from metabarcoding of *sed*aDNA from Jodavannet, Svalbard, after sequence filtering. Names in brackets represent known local species resulting from sequence match in reference libraries or BLAST result[B] when no species were identified in reference libraries.

Family/order	Taxa *sed*aDNA	Sum samples (out of 41)	Max. repeats (out of 7)	Sum repeats (out of 287)	Sum reads	Unique sequences assigned	Therm. (Elvebakk, 1989)	Bioclimatic subzone
Vascular plants								
Asteraceae	*Asteraceae*	4	5	8	1235	1 (a)		
	Arnica (***angustifolia***)	3	2	4	2212	1 (a)	II	C(s)
Brassicaceae	*Brassicaceae*	1	2	2	2267	1 (b)		
	Braya (***glabella ssp. purpurascens***)	4	6	11	1420	1 (a)	IV	A(r)
	Cardamine (***bellidifolia***)	4	4	9	501	1 (a)	V	A(f)
	Cochlearia (***groenlandica***)	3	5	7	2112	1 (a)	V	A(f)
	Draba (***arctica***, ***oblongata***)	7	3	11	4380	1 (a)	III, NA	A(f)
	Draba sp.	9	6	15	9846	1 (a)		
Caryophyllaceae	***Cerastium*** (*alpinum*, ***arcticum***, ***regelii***)	6	4	11	997	1 (a)	II, V, V	B(r), A(f), A(f)
	Minuartia rubella	4	2	5	631	1 (a)	V	A(f)
	Sagina (*caespitosa*, ***nivalis***)	5	3	8	1389	1 (a)	V, II	C(s), A(r)
	Silene acaulis	7	5	14	1850	1 (a)	IV	A(s)
	Stellaria (***longipes***)	5	6	14	614	1 (a)	V	A(f)
Cyperaceae	***Carex lachenalii***	1	4	4	3316	1 (a)	II	C(s)
	Carex (*glareosa, marina, ursina*)	1	2	2	400	1 (a)	II, I, IV	C(r), C(s), B(r)
	Carex (***nardina***, ***rupestris***)	6	7	25	1524	1 (a)	III, IV	B(r)
	Carex (***parallela***)	4	5	8	1840	1 (a)	II	C(s)
	Carex[B] (***saxatilis***)	4	4	11	328	1 (a)	II	C(s)
Equisetaceae	***Equisetum*** (***arvense***)	14	7	26	18198	1 (a)	IV	A(r)
	Equisetum (***variegatum***, *scirpoides*)	11	2	13	1306	1 (a)	IV, II	A(r), C(s)
Ericaceae	***Cassiope tetragona***	19	18	93	7487	3 (a, b)	II	C(f)
	Empetrum (***nigrum***)	15	6	31	23812	1 (a)	II	B(r)
Juncaceae	***Juncus biglumis***	6	6	19	3463	1 (a)	V	A(f)
	Luzula (*arcuata*, ***confusa***, ***nivalis***, *wahlenbergii*)	7	7	31	2517	1 (a)	II, V, V, I	C(r), A(f), A(f), C(s)
Lycopodiaceae	***Huperzia*** (***arctica***)	2	2	3	2483	1 (a)	III	B(s)
Orobanchaceae	***Pedicularis***[B] (***dasyantha/hirsutha***)	5	5	15	805	2 (a)	II, IV	B(r), A(r)
Papaveraceae	***Papaver*** (***dahlianum***, *cornwallisense*)	9	6	27	34204	1 (a)	V, NA	A(f)
Poaceae	*Calamagrostis neglecta*, ***purpurascens***)	2	5	6	176	1 (a)	II, IV[a]	C(s), B(r)
	Deschampsia (cespitosa, ***sukatschewii***)	3	4	7	299	1 (a)	NA, II	C(ca), C(s)
	Festuca (***baffinensis***, *brachyphylla, edlundiae, hyperborea*, ***ovina***, ***rubra***)	8	12	44	9479	2 (a, b)	III, IV, NA, IV, NA, IV	B(s), A(r), A(r), A(s), C(r), B(s)
	Phippsia algida	5	3	7	1692	1 (a)	V	A(f)
	Poinae (*Arctophila fulva*, ***Dupontia fisheri***)	7	5	15	1445	1 (a)	IV, V	B(s), A(r)
Polygonaceae	***Bistorta vivipara***	25	7	120	116236	1 (a)	V	A(f)
	Oxyria digyna	18	7	57	23779	1 (a)	V	A(f)
Polypodiales	***Cystopteris*** (***fragilis***)	4	6	9	21283	1 (a)	I	B(r)
Ranunculaceae	***Ranunculus***[B] (***hyperboreus***)	2	6	9	3264	3 (a)	V	A(r)
Rosaceae	***Dryas*** (***octopetala***)	18	7	100	231992	1 (a)	IV	B(r)
	Potentilla sp.	10	13	60	43111	2 (a, b)		
Salicaceae	*Salix (herbacea, lanata*, ***polaris***, ***reticulata***)	24	7	118	494575	1 (a)	II, I, V, II	B(r), C(r), A(r), C(s)
Saxifragaceae	***Micranthes*** (***hieraciifolia***, ***tenuis***)	10	5	18	1321	1 (a)	IV, V	B(r), A(s)
	Micranthes (***nivalis***, ***tenuis***)	10	3	17	795	1 (a)	V	A(s)
	Saxifraga (***cernua***, *hyperborea, rivularis*)	10	5	30	10162	1 (a)	V, V, NA	A(f), A(f), A(r)
	Saxifraga cernua	10	7	45	9441	1 (b)	V	A(f)
	Saxifraga cespitosa	8	2	10	4540	1 (a)	V	A(f)
	Saxifraga oppositifolia	25	7	105	292727	1 (a)	V	A(f)
	Saxifraga sp.	25	12	105	27412	5 (b)		
Algae								
Closteriaceae	*Closterium baillyanum*	9	7	29	139905	1 (b)		
Desmidiaceae	*Cosmarium botrytis*	17	7	57	22787	1 (b)		
Desmidiaceae	*Staurastrum punctulatum*	2	2	3	155	1 (b)		
Monodopsidaceae	*Nannochloropsis* sp.	21	7	94	512693	1 (b)		
Oocystaceae	*Neglectella solitaria*	4	2	5	357	1 (b)		
Bryophytes								
Andreaeaceae	*Andreaea nivalis*	1	2	2	104	1 (a)		
Bartramiaceae	Bartramiaceae (***Philonotis tomentella***, *P. fontana, Conostomum tetragonum*)	5	3	9	163	1 (a)		
Bryaceae	Bryaceae (*Plagiobryum zieri, P. demissum, Bryum wrightii*)	5	7	16	11746	1 (a)		
	Bryum (*arcticum,elegans*, ***pseudotriquetrum***)	16	7	41	19871	1 (a)		
	Bryum pallens	3	5	7	990	1 (a)		
Dicranaceae	*Dicranum (spadiceum, scoparium, groenlandicum*)	3	3	6	1358	1 (a)		
	Distichium (***capillaceum***, *inclinatum*)	8	3	10	1012	1 (a)		
Encalyptaceae	*Encalypta* (*rhaptocarpa, streptocarpa*)	4	2	5	103	1 (a)		
Hypnales	5 species[b]	20	17	71	54591	4 (a)		

Table 2 (*continued*)

Family/order	Taxa *sed*aDNA	Sum samples (out of 41)	Max. repeats (out of 7)	Sum repeats (out of 287)	Sum reads	Unique sequences assigned	Therm. (Elvebakk, 1989)	Bioclimatic subzone
Polytrichaceae	8 species[c]	13	7	38	25955	1 (a)		
Pottiaceae	(*Tortella fragilis, Gymnostomum aeruginosum, Hymenostylium recurvirostrum*)	1	2	2	207	1 (a)		
Timmiaceae	*Timmia* (*norvegica, austriaca*)	5	2	8	1825	1 (a)		
Sum:	*65*			*1712*	*2218623*	*77*		

For DNA sequences matching to genus or multiple species, the Svalbard representatives are given in brackets. Bold vascular (Eidesen et al., 2018) and bryophyte (https://artsdatabanken.no/) species have known current occurrence in Ringhorndalen. Nomenclature follows the Panarctic Flora (PAF) checklist for vascular plants (Elven et al., 2011), tropicos.org for bryophytes (Missouri Botanical Garden, 2018) and Guiry and Guiry (2018) for algae. All sequences have 100% match with one of the reference libraries *arctborbryo* (a) or *embl* (b). Where possible, division of species into known thermal groups is according to Elvebakk (1989) (I=Strongly thermophilous, II = Distinctly thermophilous, III=Moderately thermophilous, IV=Weakly thermophilous, and V=Temperature indifferent), [a]otherwise derived from PAF (Elven et al., 2011). Northernmost bioclimatic subzone (A = Arctic polar desert, B = northern Arctic tundra, C = middle Arctic tundra) where the species occurs as rare (r), scattered (s), frequent (f) or casual adventive (ca) at present, follows the Panarctic Flora checklist (Elven et al., 2011). Where several species are listed, the thermal groups and bioclimatic subzones are listed in the respective order, but only once if the same classification applies to all species. [b]Hypnales is possibly ***Scorpidium cossonii***/*revolvens/scorpioides*, *Pseudocalliergon turgescens* and/or ***Tomentypnum nitens*** according to present day flora. [c]Polytrichaceae is possibly *Polytrichastrum sexangulare*, *Polytrichum hyperboreum/commune/juniperinum/strictum*, *Psilopilum cavifolium/laevigatum* or *Pogonatum urnigerum*.

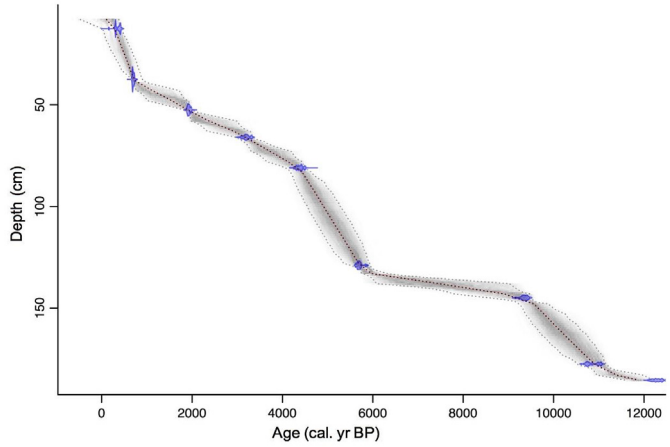

Fig. 2. Bayesian age-depth model for the nine calibrated ^{14}C ages (blue) from JVP1 in Jodavannet, Svalbard. The lines show the age-depth curve with the best model from weighted average of the mean (red), more likely calibrated ages (darker grey) and the 95% confidence interval (outer stippled grey lines).

4.2. Lithostratigraphy

Changes in the depositional environment were revealed based on lithology, geochemical composition and organic content (Fig. 3). Four lithological units (LU 1–4) were identified.

LU 1: Core depth 186-176 cm, *c.* 11,900-10,800 cal. yr BP

LU 1 consists of light grey to very light green, clayey silt with interlaminated organic material. We interpret LU 1 as deposited by minerogenic-rich sedimentation driven by inflow of glacial meltwater across the eastern threshold of the Jodavannet catchment.

LU 2: Core depth 176-81 cm, *c.* 10,800-4300 cal. yr BP

There is a large reduction in indicators of glacially derived minerogenic input (MS, X-ray derived density and Ti), increasing LOI, and a peak in Ca at the transition from LU 1 to LU 2. LU 2 consists of well-stratified tan brown to olive grey, silty gyttja with sporadic interlaminated organic material. The bedding transitions from well-stratified to crudely stratified from the base of the unit towards the top. We interpret LU 2 as deposited by the accumulation of organic material with minimal minerogenic input.

LU 3: Core depth 81-19 cm, *c.* 4300–400 cal. yr BP

LU 3 consists of dark tan to very dark brown silty gyttja with organic-rich lamina interrupted by occasional light tan silt beds. The XRF profiles are relatively unstable and variable, and LOI decreases gradually. We interpret LU 3 as deposited by accumulation of organic material interrupted by increasing episodic minerogenic input.

LU 4: Core depth 19-0 cm, after *c.* 400 cal. yr BP

LU 4 consists of light grey to light tan weakly laminated silty fine sand with occasional laminae of brown organic material. We interpret LU 4 as deposited by minerogenic-rich sedimentation with minimal biogenic accumulation. The sediment source is interpreted as nival or aeolian, or a combination of both.

4.3. SedaDNA analysis

During bioinformatic processing, the number of reads and sequences were reduced from an initial raw count of *c.*16.7 million paired-end reads to *c.*11 million reads of which there were 7158 unique sequences (after OBITools, but prior to R filtering). After R filtering, the resulting counts were 2,396,240 reads represented by 77 unique sequences. Full details of the bioinformatic approach and the number of reads and sequences remaining after each step are given in Table A (Appendix A). The resulting sequences were assigned to vascular plants (73.8%), algae (7.7%) and bryophytes (18.5%) from 65 different taxa (Table 2).

No taxa were present in all samples. The most abundant vascular plants in the *sed*aDNA record were *Bistorta vivipara* (61%), *Saxifraga* sp. (61%), *Saxifraga oppositifolia* (61%), and *Salix* (59%) (based on overall presence in samples; Table 2). *Cassiope tetragona* (46%), *Oxyria digyna* (44%) and *Dryas octopetala* (44%) were also frequently detected, followed by *Empetrum nigrum* (37%), *Equisetum arvense* (34%), and *Equisetum variegatum/scirpoides* (27%).

Three significant *sed*aDNA zones were found based on the constrained hierarchical cluster analysis of Bray-Curtis community distance on PCR replicates per sample (Figs. 4 and 5 and Fig. B, Appendix A) and the comparison with a broken stick model

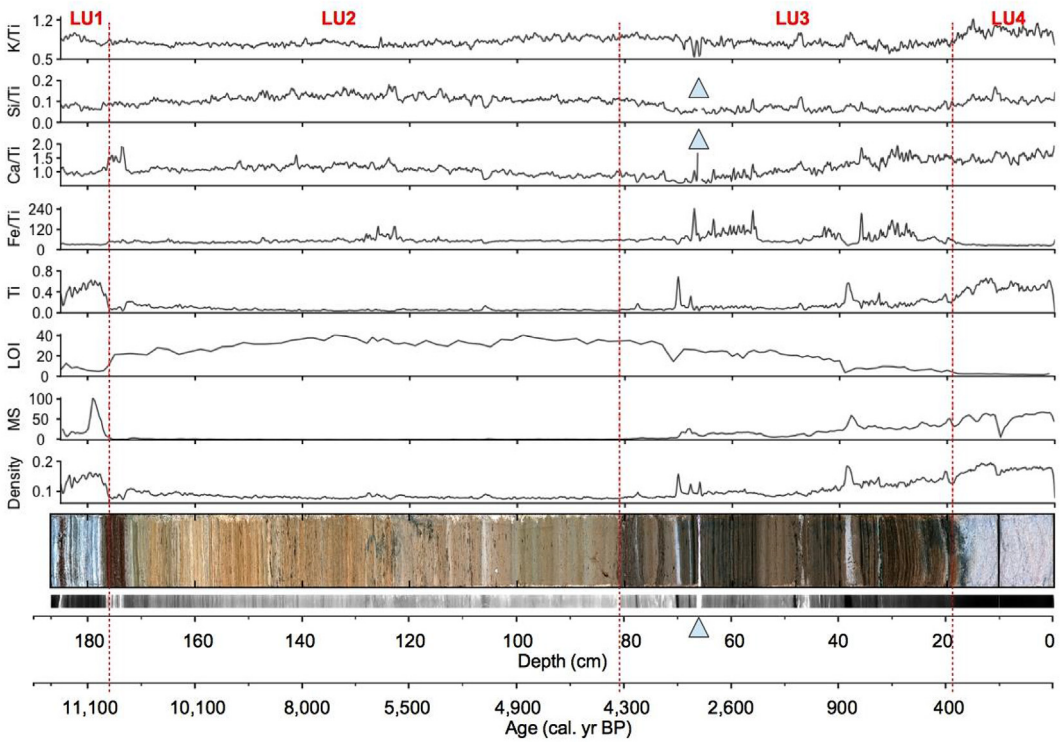

Fig. 3. Sediment properties and elemental profiles for Jodavannet, Svalbard. Weighted moving averages (n = 5) of selected element profiles measured by XRF are given as a ratio to Ti. The Ti profile is normalized against Rh coh + Rh inc. Loss-on-ignition is given as a percentage of dry sediment weight after ignition at 550 °C. Magnetic susceptibility (MS) is depicted as weighted moving average (n = 5). Density is a proxy from Rh coh/Rh inc. All graphs and optical and radiographic images are plotted against core depth (cm) and corresponding age (cal. yr BP). The dashed lines indicate the lithostratigraphic units (LU 1-4) described in the text. The filled triangles mark extreme peaks in the Si/Ti and Ca/Ti ratios that are outside the depicted range, and the corresponding depth.

distribution (Fig. C, Appendix A). The greatest assembly distance among adjacent samples was between sample depth 78 and 90 cm (*c.* 4400 cal. yr BP), followed by 154 and 156 cm (*c.* 9900 cal. yr BP), making the youngest zone the most distinct. The identified *sed*aDNA zones correspond to visually marked transitions in the composition of *sed*aDNA taxa (Figs. 4 and 5 and Table B, Appendix A).

4.3.1. SedaDNA zone 1: sample depth 185-156 cm, c. 11,700-9900 cal. yr BP (n = 15)

Most of the taxa dominating in the oldest part of the sediment core were herbaceous, non-graminoid vascular plants and bryophytes typical of wet habitats, e.g. *Ranunculus hyperboreus*, *Saxifraga cernua/hyperborea/rivularis*, Hypnales and Pottiaceae (see Table 2 for species). Overall, we found taxa with very different ecological characteristics, for example *Saxifraga oppositifolia* (widely distributed generalist), *Saxifraga cespitosa* (relatively drought-tolerant), *Papaver cornwallisense/dahlianum* (hardy pioneer), and *Cystopteris fragilis* (strong thermophile, sensu Elvebakk, 1989).

There was a marked reduction in vascular plant and bryophyte taxa around 10,600 cal. yr BP, while algae became dominant (especially *Nannochloropsis* sp.). The first occurrence of the distinct thermophiles *Arnica angustifolia* (*c.* 10,200 cal. yr BP) and *Empetrum nigrum* (*c.* 10,400-10,200 cal. yr BP) appeared. The overall taxonomic richness in *sed*aDNA zone 1 was 65% of all taxa present (26 vascular, 8 bryophyte and 4 algal taxa) with an average of 2.7 plant taxa per sample. The taxonomic diversity was lower from 10,600 cal. yr BP onwards. Some taxa were exclusively found in *sed*aDNA zone 1, namely *Carex marina/ursina/glareosa*, *Ranunculus hyperboreus*, Pottiaceae and *Neglectella solitaria*.

4.3.2. SedaDNA zone 2: sample depth 155-90 cm, c. 9900-4600 cal. yr BP (n = 18)

The *sed*aDNA record in zone 2 was still dominated by *Nannochloropsis* sp. until *c.* 8200 cal. yr BP, but overall algal read abundance was reduced compared to the youngest part of *sed*aDNA zone 1. *Nannochloropsis* sp. also occurred sporadically *c.* 5600–4600 cal. yr BP, and two other algal taxa (*Cosmarium botrytis* and *Closterium baillyanum*) were present *c.* 9100–8,800, 5400-5200 and 4900 cal. yr BP. There were relatively few bryophytes, with Hypnales as the most abundant bryophyte taxa.

The percentage of vascular plant taxa was similar between *sed*aDNA zone 1 and 2 (63% and 60%, respectively). The dwarf shrubs *Empetrum nigrum* and *Salix* were relatively dominant throughout *sed*aDNA zone 2, while *Dryas octopetala* and *Cassiope tetragona* followed *c.* 6400 and 4900 cal. yr BP, respectively. Among the herbs, *Bistorta vivipara*, *Saxifraga oppositifolia*, *Saxifraga* sp., and *Oxyria digyna* dominate. Graminoids were generally infrequent, but a few thermophilous sedges were present. The distinctly thermophilous *Carex lachenalii* was recorded exclusively in *sed*aDNA zone 2, *c.* 9770 cal. yr BP, and the distinctly thermophilous *Carex parallela* occurred for the first time in the record *c.* 5300 cal. yr BP. Additionally, the moderately thermophilous club moss *Huperzia arctica* occurred exclusively in this zone, *c.* 5500 cal. yr BP. The thermophilous species (*sensu* Elvebakk, 1989) *Cystopteris fragilis* (strongly thermophilous) and *Arnica angustifolia* (distinctly thermophilous) reappeared in the record *c.* 5300 and *c.* 4900 cal. yr BP, respectively. The widespread Arctic-alpine species *Silene acaulis* occurred for the first time in the record *c.* 8200 cal. yr BP. The overall taxonomic richness in *sed*aDNA zone 2 (~57% of all detected taxa; 29 vascular, 5 bryophyte and 3 algae; average 2.5 plant taxa per sample) was similar to the previous zone.

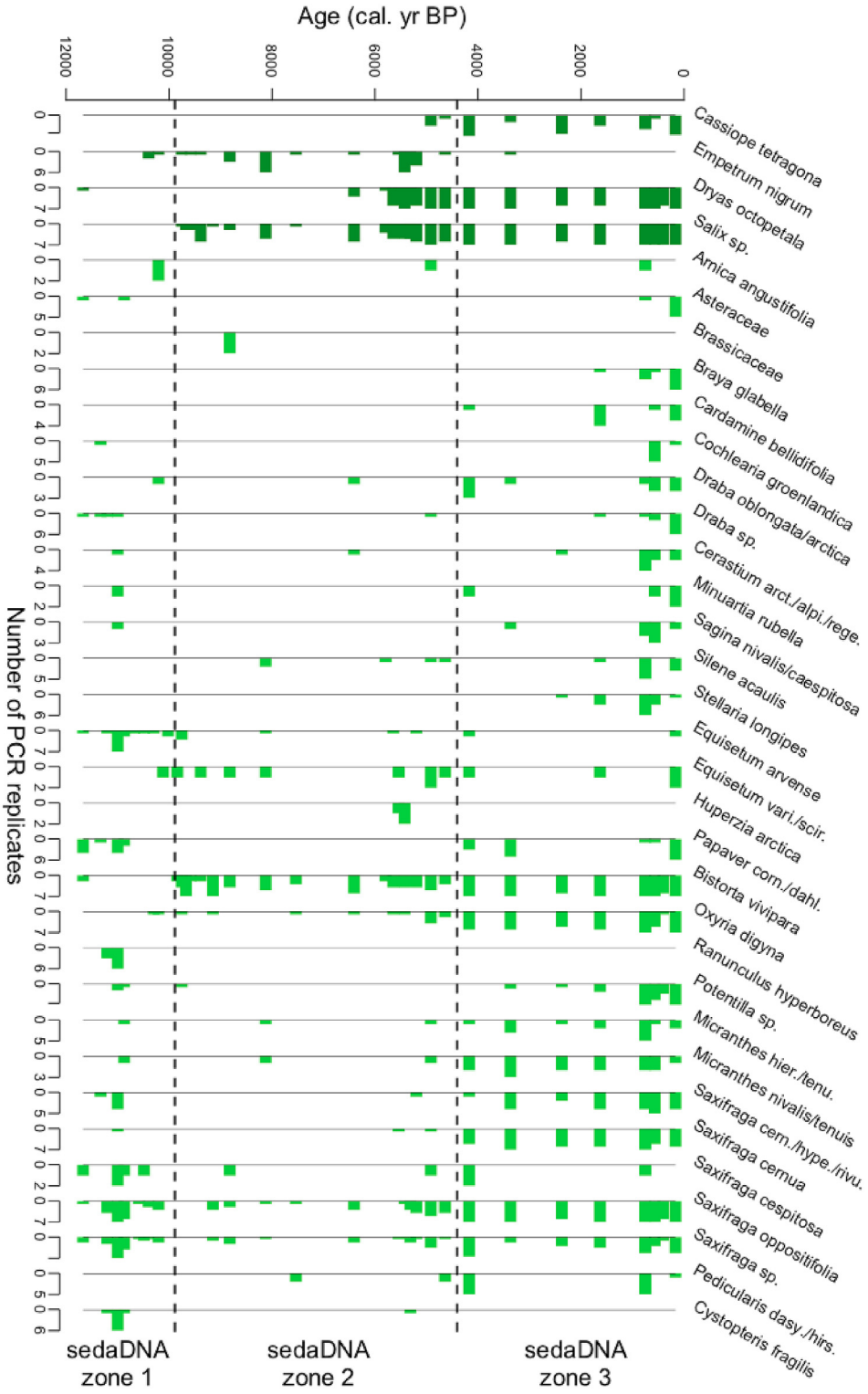

Fig. 4. Stratigraphic diagram of shrubs (dark green) and herbs (light green) identified from *sed*aDNA in Jodavannet, Svalbard. The diagram is created with the *strat.plot* function (*rioja 0.9-15.1*) and depicts the number of PCR replicates of identified taxa (bars; x-axis) corresponding to sample age (cal. yr BP; y-axis). The hatched lines mark four *sed*aDNA zones (1–3) identified from constrained (by sample order) hierarchical clustering of species community dissimilarity (Bray-Curtis) of all taxa. For full taxa names see Table 2. Note that the following taxa consist of several sequences, thus they potentially have >7 PCR replicates: *Saxifraga* sp. (5) and *Festuca* sp. (2), *Ranunculus hyperboreus* (3) and *Pedicularis dasyantha/hirsuta* (2).

4.3.3. SedaDNA zone 3: sample depth 79-8 cm, c. 4200-150 cal. yr BP (n = 8)

Most vascular plant taxa were present in *sed*aDNA zone 3 (~85%), and several occurred for the first time in the record (*Braya glabella*, *Cardamine bellidifolia*, *Stellaria longipes*, *Carex saxatilis*, *Luzula*, *Calamagrostis*, *Deschampsia* and Poinae). Graminoids had a marked increase with 10 out of 12 taxa present. Dwarf shrubs were consistently represented throughout *sed*aDNA zone 3 with

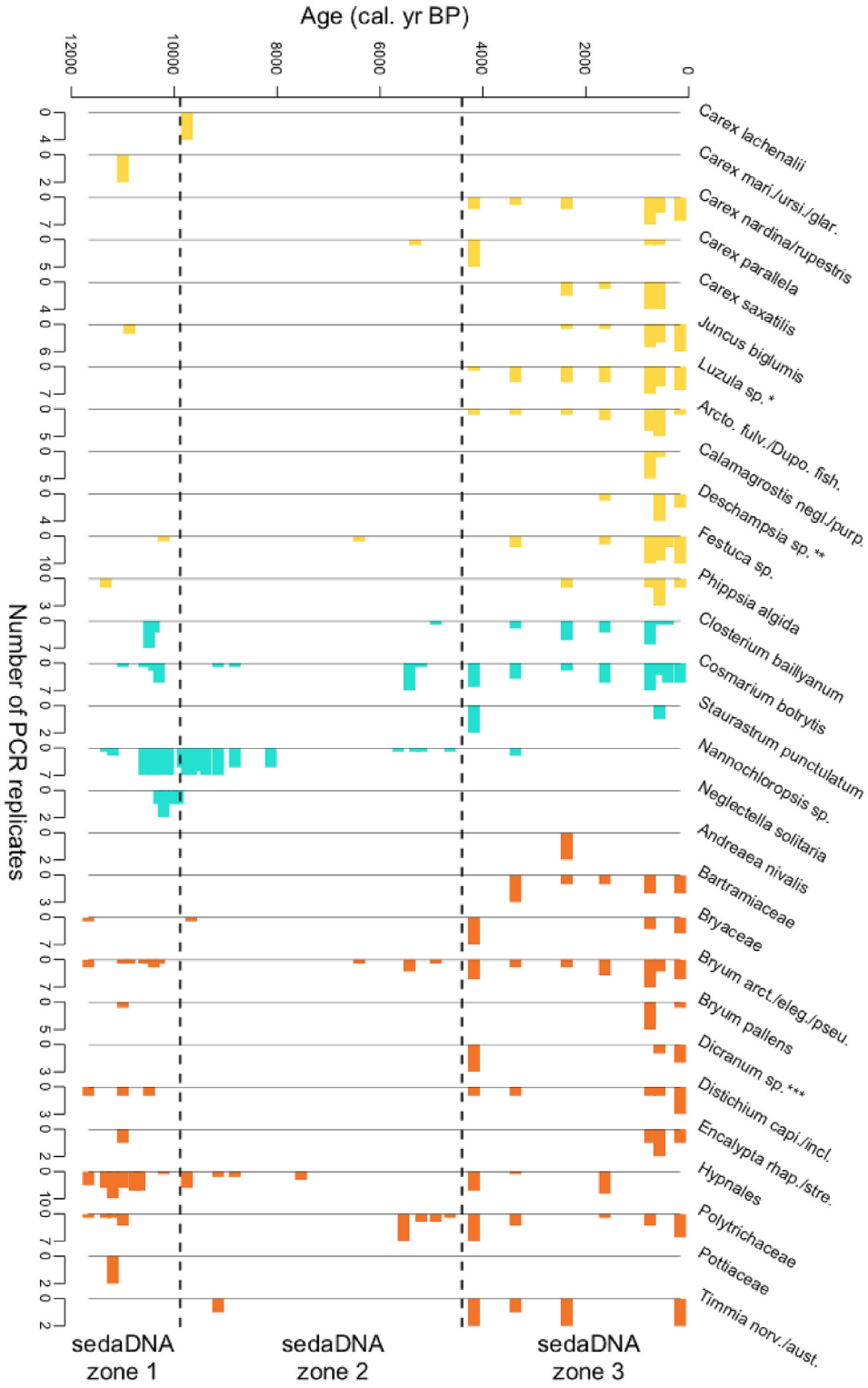

Fig. 5. Stratigraphic diagram of graminoid (yellow), algal (turquoise) and bryophyte (orange) taxa identified from *sed*aDNA in Jodavannet, Svalbard. The diagram is created with the *strat.plot* function (*rioja 0.9-15.1*) and depicts the number of PCR replicates of identified taxa (bars; x-axis) corresponding to sample age (cal. yr BP; y-axis). The hatched lines mark four *sed*aDNA zones (1–3) identified from constrained (by sample order) hierarchical clustering of species community dissimilarity (Bray-Curtis) of all taxa. For full taxa names see Table 2. Note that Hypnales consists of four unique sequences, hence they potentially have >7 PCR replicates. **Luzula* sp. = *Luzula confusa/wahlenbergii/nivalis/arcuate*, ***Deschampsia* sp. = *Deschampsia sukatschewii/cespitosa/brevifolia* and ****Dicranum* sp. = *Dicranum spadiceum/fuscescens/groenlandicum*.

relatively high read abundance. Several thermophilous taxa were present (*Arnica angustifolia*, *Calamagrostis*, *Carex parallela*, *C. saxatilis*, *Cassiope tetragona* and *Empetrum nigrum*), especially *c.* 4200–560 cal. yr BP. After this period, the thermophilous indicators decreased. There was also a pronounced change in dwarf shrubs, as *Cassiope tetragona* was consistently present in almost all samples,

while *Empetrum nigrum* disappeared from the record after *c.* 3400 cal. yr BP.

Algal and bryophyte taxa were also abundant with almost all taxa present, and *sed*aDNA zone 3 was the zone with the overall highest total and average taxonomic richness: ~86% of all detected taxa were present (41 vascular, 11 bryophyte and 4 algae), with an average of 7 taxa per sample.

4.3.4. Comparison to current vegetation

More than 50% of taxa found in the sediment record were not registered during surveys of contemporary vegetation close to the lake (Table C, Appendix A). However, the majority of the inferred taxa are found in the Ringhorndalen valley (taxa in bold, Table 2). Only *Arctophila fulva* and *Calamagrostis neglecta* have not been found in Ringhorndalen before, but these taxa are found elsewhere in Svalbard. *Draba* sp., Asteraceae and Brassicaceae had too low taxonomic resolution for classification of local presence, because the taxa included both local and non-local representatives.

4.4. Comparison between lithology and vegetation records

The stratigraphic zones identified for each data record were largely congruent (Fig. 6): *Sed*aDNA zone 1 was comparable to LU 1. LU 2 comprised a small part of *sed*aDNA zone 1 and the complete *sed*aDNA zone 2. The transitions to *sed*aDNA zone 3 and LU 3 appeared largely synchronous. LU 4 was not identified as significantly distinct in the *sed*aDNA record ($n = 2$ within that lithological unit). Together, the *sed*aDNA zones and lithostratigraphic units defined three characteristic time periods based on environmental differences (Fig. 6).

5. Discussion

5.1. Holocene development of vegetation and climate

5.1.1. Rapid colonization during the late glacial and Early Holocene (c. 11,900–9900 cal. yr BP)

The high proportion of species recorded in this early period (>50%) and relatively high assemblage turnover around 10,600 cal. yr BP occurring over a relatively short time span (~2000 years) could be due to either an early deglaciation or rapid colonization (Figs. 4 and 5). We do not know the exact timing of deglaciation at the site, but cosmogenic exposure ages from Dellingstupa (135 m a.s.l. and 145 m a.s.l.; Fig. 1c) suggest ice-free conditions as early as 14,600-13,800 ± 1000 yr ago (Hormes et al., 2013). The lithology of LU 1 (Fig. 3) reflects minerogenic-rich sedimentation, suggesting inflow of glacial meltwater across the eastern threshold of the Jodavannet catchment (Fig. 1). This indicates the presence of glaciers in the catchment. Thus, the site was most likely rapidly colonized at the time that glaciers left the watershed. Recent studies of lacustrine and raised marine sediments from northern and western Spitsbergen also suggest glacier retreat and species colonization during the late glacial (Gjerde et al., 2017; Farnsworth et al., 2018; Larsen et al., 2018). Diverse pollen records are known from further north in Wijdefjorden at Lake Strøen and Nordaustlandet (both Hyvärinen, 1970), Edgeøya (Bennike and Hedenäs, 1995), and the more southern Bjørnøya (Hyvärinen, 1970; Wohlfarth et al., 1995). This includes several of the taxa we recorded, such as *Ranunculus*, *Papaver*, and *Saxifraga*. High frequency of immigration to Svalbard has also been interpreted based on studies of modern DNA (Alsos et al., 2007). Mangerud and Svendsen (2018) suggested that the August sea-

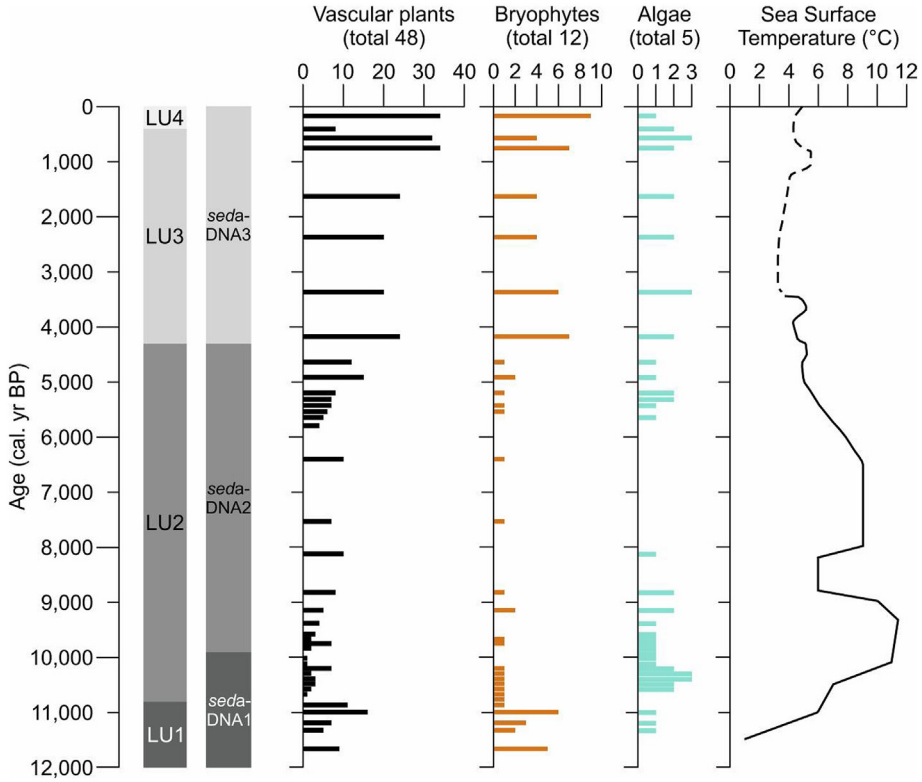

Fig. 6. Details of the *sed*aDNA samples (modelled median age, lithological unit (LU) statistically identified *sed*aDNA zone, and the number of taxa within vascular plants, bryophytes, and algae obtained from *sed*aDNA analysis). Reconstructed sea-surface temperature for the west coast of Spitsbergen from Mangerud and Svendsen (2018) is shown to the right.

surface temperatures were up to about 6 °C warmer than present between 11,000 and 10,500 cal. yr BP. Our identification of the strongly thermophilous species *Cystopteris fragilis* in the *sed*aDNA record *c.* 11,200-10,900 cal. yr BP further suggests that this was a period considerably warmer than today, which allowed rapid establishment of a diverse flora.

The marked transition from LU 1 to LU 2, *c.* 10,800 cal. yr BP (Fig. 3), indicates an abrupt termination of glacial meltwater inflow. This likely changed the nutrient conditions of the lake causing the recorded algal bloom (Fig. 5). The relative decrease of bryophytes and vascular plants at this time is likely attributed to the dominance of algal DNA, as this may cause underestimation of other taxa (Alsos et al., 2018a). Indeed, the appearance of more thermophilous species like *Empetrum* and *Arnica* suggests that the climate was warmer than today. This is also in accordance with a rise in sea-surface temperature (Hald et al., 2004; Mangerud and Svendsen, 2018) and lake-water temperatures (van der Bilt, 2016).

5.1.2. Dry and warm middle Holocene (9900–4300 cal. yr BP)

Our records suggest climatically stable, dry and warm conditions throughout most of the middle Holocene (from the beginning of *sed*aDNA zone 2 to the onset of LU 3 and *sed*aDNA zone 3). The *sed*aDNA record shows a relatively species-rich vegetation with the establishment of several dwarf-shrubs and herbs common in Svalbard today, and a consistent presence of thermophilous indicator taxa (Fig. 6). The low catchment erosion intensity inferred from the lithostratigraphical record strengthens this interpretation. The August sea-surface temperatures are suggested to have been about 4 °C higher than present from *c.* 8000 to 6500 cal. yr BP, followed by a gradual decrease in temperature until present day levels around 3500 cal. yr BP (Mangerud and Svendsen, 2018). The vegetation and lithological reconstructions from Jodavannet support these findings. This is also a period with increased pollen production (Hyvärinen, 1968; 1969, 1970), peat formation (Göttlich and Hornburg, 1982; van der Knaap, 1989), and rich macrofossil records (Birks, 1991; Alsos et al., 2016). On the contrary, Mangerud and Svendsen (2018) describe cooler conditions in Svalbard between *c.* 8800 and 8200 cal. yr BP. This is not apparent in our data, potentially because the two samples we have are from just before and just after, rather than from this cooler period.

Dryas appeared around 6400 cal. yr BP, suggesting a shift in vegetation from moist snowbed communities dominated by *Salix polaris* and *Bistorta vivipara* to the inclusion of semi-dry heath vegetation with *Saxifraga oppositifolia* and *Dryas octopetala* (Elvebakk, 1994). Similarly, Alsos et al. (2016) revealed a shift towards more dry tolerant taxa with an increase of *Dryas* after *c.* 6400 cal. yr BP in western Spitsbergen. This shift could be explained by a mid-Holocene increase in Fram Strait sea-ice extent, resulting in reduced moisture supply to Svalbard (Müller et al. 2012). Mollusc data indicate a cooling from 6500 cal. yr BP (Mangerud and Svendsen, 2018), suggesting a combined effect of cooling and drying.

Reestablishment and/or confident detection of thermophilous indicator species, such as *Empetrum, Cystopteris fragilis* and *Arnica angustifolia*, from *c.* 5500 to 5000 cal. yr BP, reflects high temperatures, consistent with suggestions by Luoto et al. (2017). This is also a period with high taxonomic richness recorded in *sed*aDNA data from a western Spitsbergen lake sediment core (Alsos et al., 2016).

5.1.3. Neoglacial environmental changes in the Late Holocene (c. 4300–150 cal. yr BP)

The lithology and *sed*aDNA data show a distinct shift *c.* 4300 cal. yr BP, reflecting the onset of the Neoglacial period (4200 cal. yr BP; Fig. 3; Farnsworth, 2018; Bradley and Bakke, 2019). This period is characterized by an increasing amount of minerogenic material interrupting the accumulation of organic material and a shift in vegetation, combined with the first appearance of many new taxa (Figs. 3–5). The overall increase in the number of taxa identified from *sed*aDNA can be explained by: 1) better DNA quality in recent samples due to younger age and/or cooler conditions during deposition, favouring preservation, 2) the cumulative effect of colonization over time, 3) sediment properties and/or 4) more frequent stochastic dispersal caused by extreme weather events. Some studies report higher diversity in more recent than older sediments (Pansu et al., 2015; Clarke et al., 2019b). However, other studies show higher diversity in older samples and from warmer periods (Alsos et al., 2016; Zimmermann et al., 2017a; Clarke et al., 2019a). Given the lower temperatures on Svalbard relative to the majority of these other studied regions, we do not believe that age or temperature during deposition within the ranges studied here had a major impact on number of detected species. Dispersal lags may have affected arrival of some species (see below), but neither pollen, macro, nor previous DNA records from Svalbard show a clear increase in diversity over time (Hyvärinen, 1970; van der Knaap, 1989; Birks, 1991; Bennike and Hedenäs, 1995; Wohlfarth et al. 1995; Alsos et al., 2016). This suggests that colonization lags are not enough to explain the high increase in diversity in recent samples. We consider a combination of explanations 3 and 4 to be more likely. Notably, the marked increase in number of taxa from *sed*a DNA zone 2 to 3 is in concordance with a shift from algal gyttja to increased minerogenic input (LU2 to LU3). More fluctuations and laminations suggest increasingly stormy conditions, potentially with changes in main wind directions, bringing neighbouring terrestrial material into the catchment. The corresponding peaks in terrigenous input, coarse sediment signal, and white sediment colour are likely to reflect nival and/or aeolian deposition of sandy sediments (Røthe et al., 2018). More minerogenic input is often related to better DNA preservation (Torti et al., 2015). The increased diversity may thus be a direct effect of minerogenic input, potentially combined with input from outside the catchment. An increase in bryophytes combined with more variable runoff was also recorded in western Spitsbergen from around 5500 cal. yr. BP (Alsos et al., 2016), suggesting that the vegetation shift is caused by a regional change in climate.

All dwarf shrubs are common in the Late Holocene period, but *Empetrum* disappears from the record after *c.* 3400 cal. yr BP. Local extinction of this shrub may be related to more competition with *Cassiope tetragona* and *Dryas octopetala.* Experimental warming studies in Svalbard have shown that *Empetrum nigrum* is favoured by warmer conditions, whereas it is outcompeted by *Cassiope tetragona* under cooler conditions (Buizer et al., 2012). This species replacement would suggest increasingly cooler Neoglacial conditions. However, the presence of several thermophilous indicator species (i.e. *Calamagrostis*, *Cassiope tetragona*, *Carex saxatilis* and *Carex parallela*) between *c.* 750-570 cal. yr BP suggests relatively warm local conditions. These contrasting patterns can be explained by regional glacial expansion in surrounding areas combined with a favourable local microclimate, as well as the ability of clonal plants to persist for long periods of climate deterioration (Alsos et al., 2002). Today, there are favourable conditions for plant growth as well as large ice caps in close proximity to Ringhorndalen, and it is likely that these conditions developed during the Neoglacial period (Gjerde et al., 2017; Miller et al., 2017).

The lithology of LU 4 (*c.* 400 cal. yr BP; Fig. 3) indicates minerogenic-rich sedimentation with minimal biogenic accumulation. We only have two *sed*aDNA samples from LU 4, with highly

contrasting species richness (10 vs. 44 taxa). The sediment source is likely nival, aeolian, or a combination of both. DNA binds better to smaller clay particles than to sand (Torti et al., 2015). Thus, the variation in species richness between these two samples may be due to taphonomic issues in LU 4.

5.2. Future prospects and implications for conservation of species

While half of the taxa recorded were already present in the oldest samples, the total species richness almost doubles over the 12,000-year period. Arrival time may relate to climate, dispersal mode, stochastic events and/or dispersal distance (Alsos et al., 2007, 2016). One of the major dwarf shrubs of the northern hemisphere, *Empetrum*, colonized the catchment as early as 10,400 cal. yr BP, about the same time as it appears in records from eastern Greenland (Bennike et al., 1999) and northern Norway (Clarke et al., 2019a). This species has low genetic structure, suggesting broad-fronted colonization, perhaps assisted by bird dispersal (Eidesen et al., 2013; Alsos et al., 2015). As the lake catchment of Jodavannet is outside the current distribution range of *Empetrum* (Fig. 1), our *sed*aDNA records support the interpretation that current distribution represents relics of a once wider distribution (Engelskjøn et al., 2003; Alsos et al., 2007). In contrast, *Cassiope tetragona* is hardier than *Empetrum*, but not detected in the record until 4900 cal. yr BP. This species was not found in northern Greenland until 7800 cal. yr BP (Wagner et al., 2010), probably due to a long migration route from the glacial survival site in Beringia across Canada and Greenland before its appearance in Svalbard, as indicated by genetic analyses (Eidesen et al., 2007).

Although some species are only recorded in the older samples, they are not regionally extinct (Eidesen et al., 2018). For example, the thermophilous species *Cystopteris* and *Empetrum* are not found in any samples from the Neoglacial period. Thus, their current restricted distribution in the valley (Fig. 1, Eidesen et al., 2018) may represent remnants of a once larger local population, as has also been inferred for other plant taxa (Alsos et al., 2002, 2007). The heterogeneous environment, together with exceptionally favourable climatic conditions for this high latitude, have ensured long-term persistence of plant species and confirm the high conservation value of this locality.

With ongoing climatic warming, we may expect thermophilous species recorded in the *sed*aDNA (Table 2) and further in the valley (Eidesen et al., 2018) to expand. There are also a range of thermophilous taxa in the neighbouring areas of Greenland, Fennoscandia, and Russia that may colonize Svalbard (Alsos et al., 2007) and would most likely establish at sites with favourable local climate, such as Ringhorndalen. Furthermore, increasing human traffic to the region increases the risk of anthropogenic species introductions (Alsos et al., 2015). This expected expansion of thermophilous species may pose a threat to the less competitive, high-Arctic species in the region. However, Clarke et al. (2019b) found evidence of a refuge site for cold tolerant species from a 24,000-year old record from the Polar Urals. They suggest that mountainous landscapes may provide refuge sites for cold tolerant species in warmer climate. We believe that sites like Ringhorndalen, with high species richness and topographic diversity that facilitates for microclimatic variation, are important for long-term survival of both cold and warm adapted species.

6. Conclusions

Our combined geochemical and molecular evidence suggests that isolated populations of unusually thermophilous plant species found in Ringhorndalen today are relicts from a more widespread distribution during warmer Holocene periods. Our results support previous evidence of an Early Holocene warming, indicating good agreement between marine and terrestrial archives. We show that Arctic hotspots like Ringhorndalen are not only important for the biodiversity today, but may represent sites of long-term survival of species, making them an important conservation priority.

Author contributions

PBE, LH, AS, and IGA developed the idea and supervised the study; WRF and AS cored the lake; AS, WRF, SEK, AR, and LH described and interpreted the lithology and identified plant macrofossils for radiocarbon dating; SEK conducted the LOI analysis; LHV did the age-depth model; LHV and PBE did the vegetation surveys; AR and WRF did the *sed*aDNA clean sub-sampling; LHV and PDH did the *sed*aDNA analyses; LHV did the bioinformatics analyses; LHV drafted the manuscript with contributions from all co-authors.

Acknowledgements

The core-sampling field campaign, subsequent sub-sampling of sediments and macrofossils, ITRAX-scans, and radiocarbon dating were funded by the Svalbard Environmental Protection Fund (project 16/35 to WRF). Financial support for molecular analysis and field work was provided by the Svalbard Environmental Protection Fund (project 14/118 to PBE) and Jan Christensen's endowment (to LHV). IGA and PDH acknowledge support from the Research Council of Norway (Grant 250963: "ECOGEN"). We thank Johannes Sand Bolstad for field assistance, Kari Klanderud for project administration, the wider ECOGEN research group in Tromsø, including Dilli Rijal for pooling and cleaning of the PCR products and Youri Lammers for helping with bioinformatic analyses and reference libraries. Bioinformatic analyses were performed on the Abel Cluster, owned by the University of Oslo and Uninett/Sigma2, and operated by the Department for Research Computing at USIT, the University of Oslo IT-department. http://www.hpc.uio.no/. We thank Marie-Louise Siggaard-Andersen for assistance with the ITRAX-scanning of the sediment core as well as Dr. Skafti Brynjólfsson and Dr. Marc Macias-Fauria for collaboration in the field.

Appendix A. Supplementary data

Supplementary data to this article can be found online at https://doi.org/10.1016/j.quascirev.2020.106207.

References

Alsos, I., Engelskjøn, T., Brochmann, C., 2002. Conservation genetics and population history of *Betula nana*, *Vaccinium uliginosum*, and *Campanula rotundifolia* in Svalbard. Arctic Antarct. Alpine Res. 34, 408–418. https://doi.org/10.1080/15230430.2002.12003511.

Alsos, I.G., Eidesen, P.B., Ehrich, D., Skrede, I., Westergaard, K., Jacobsen, G.H., Landvik, J.Y., Taberlet, P., Brochmann, C., 2007. Frequent long-distance plant colonization in the changing Arctic. Science 316 (5831), 1606–1609. https://doi.org/10.1126/science.1139178.

Alsos, I.G., Ware, C., Elven, R., 2015. Past Arctic aliens have passed away, current ones may stay. Biol. Invasions 17, 3113–3123.

Alsos, I.G., Sjögren, P., Edwards, M.E., Landvik, J.Y., Gielly, L., Forwick, M., Coissac, E., Brown, A.G., Jakobsen, L.V., Føreid, M.K., Pedersen, M.W., 2016. Sedimentary ancient DNA from Lake Skartjørna, Svalbard: assessing the resilience of arctic flora to Holocene climate change. Holocene 26, 627–642. https://doi.org/10.1177/0959683615612563.

Alsos, I.G., Lammers, Y., Yoccoz, N.G., Jorgensen, T., Sjögren, P., Gielly, L., Edwards, M.E., 2018a. Plant DNA metabarcoding of lake sediments: How does it represent the contemporary vegetation. PloS One 13 (4), e0195403. https://doi.org/10.1371/journal.pone.0195403.

Alsos, I.G., Elven, R., Arnesen, G., Sandbakk, B.E., 2018b. The Flora of Svalbard. Available at: http://svalbardflora.no.

Artskart artsdatabanken no, 2019. Registration Data from: Svalbardflora.Net,

Naturhistorisk Museum - UiO, Tromsø Museum – Universitetsmuseet. Accessed from Artskart. https://artskart.artsdatabanken.no. (Accessed 7 December 2019).
Balascio, N.L., Zhang, Z., Bradley, R.S., Perren, B., Dahl, S.O., Bakke, J., 2011. A multi-proxy approach to assessing isolation basin stratigraphy from the Lofoten Islands, Norway. Quat. Res. 75, 288–300. https://doi.org/10.1016/j.yqres.2010.08.012.
Bennett, K.D., 1996. Determination of the number of zones in a biostratigraphical sequence. New Phytol. 132, 155–170.
Bennike, O., Hedenäs, L., 1995. Early Holocene land floras and faunas from Edgeøya, eastern Svalbard. Polar Res. 14, 205–214.
Bennike, O., Björck, S., Böcher, J., Hansen, L., Heinemeier, J., Wohlfarth, B., 1999. Early Holocene plant and animal remains from North-east Greenland. J. Biogeogr. 26, 667–677.
Berglund, B.E., Barnekow, L., Hammarlund, D., Sandgren, P., Snowball, I.F., 1996. Holocene forest dynamics and climate changes in the Abisko area, northern Sweden: the Sonesson model of vegetation history reconsidered and confirmed. Ecol. Bull. 45, 15–30.
van der Bilt, W., 2016. Towards a Process-Based Understanding of Holocene Polar Climate Change. Using Glacier-Fed Lake Sediments from Arctic Svalbard and Antarctic South Georgia. Doctoral thesis, University of Bergen.
Birkeland, S., Skjetne, I.E.B., Brysting, A.K., Elven, R., Alsos, I.G., 2017. Living on the edge: conservation genetics of seven thermophilous plant species in a High Arctic archipelago. AoB PLANTS 9, plx001. https://doi.org/10.1093/aobpla/plx001.
Birks, H.H., 1991. Holocene vegetational history and climatic change in west Spitsbergen-plant macrofossils from Skardtjørna, an Arctic lake. Holocene 1, 209–218.
Birks, H.H., Paus, A., Svendsen, J.I., Alm, T., Mangerud, J., Landvik, J.Y., 1994. Late Weichselian environmental change in Norway, including Svalbard. J. Quat. Sci. 9, 133–145. https://doi.org/10.1002/jqs.3390090207.
Blaauw, M., Christen, J.A., 2011. Flexible paleoclimate age-depth models using an autoregressive gamma process. Bayesian Anal. 6, 457–474. https://doi.org/10.1214/ba/1339616472.
Boyer, F., Mercier, C., Bonin, A., Le Bras, Y., Taberlet, P., Coissac, E., 2016. obitools: a unix-inspired software package for DNA metabarcoding. Mol. Ecol. Resour. 16, 176–182. https://doi.org/10.1111/1755-0998.12428.
Bradley, R.S., Bakke, J., 2019. Is there evidence for a 4.2 ka BP event in the northern North Atlantic region? Clim. Past 15, 1665–1676 rg\10.5194\cp-15-1665-2019 \o org/10.5194/cp-15-1665-2019.
Buizer, B., Weijers, S., van Bodegom, P.M., Alsos, I.G., Eidesen, P.B., van Breda, J., de Korte, M., van Rijckevorsel, J., Rozema, J., 2012. Range shifts and global warming: ecological responses of *Empetrum nigrum* L. to experimental warming at its northern (high Arctic) and southern (Atlantic) geographical range margin. Environ. Res. Lett. 7, 025501.
CAFF, 2013. Arctic Biodiversity Assessment. Status and Trends in Arctic Biodiversity. Conservation of Arctic Flora and Fauna, Akureyri.
Clarke, C.L., Edwards, M.E., Brown, A.G., Gielly, L., Lammers, Y., Heintzman, P.D., Ancin-Murguzur, F.J., Bråthen, K.A., Goslar, T., Alsos, I.G., 2019a. Holocene floristic diversity and richness in northeast Norway revealed by sedimentary ancient DNA (seda DNA) and pollen. Boreas 48, 299–316.
Clarke, C., Edwards, M., Gielly, L., Ehrich, D., Hughes, P., Morozova, L., Haflidason, H., Mangerud, J., Svendsen, J., Alsos, I., 2019b. Persistence of arctic-alpine flora during 24,000 years of environmental change in the Polar Urals. Sci. Rep. 9, 1–11.
Croudace, I.W., Rindby, A., Rothwell, R.G., 2006. ITRAX: description and evaluation of a new multi-function X-ray core scanner. Geol. Soc., Lond., Spec. Publ. 267, 51–63. https://doi.org/10.1144/GSL.SP.2006.267.01.04.
Cuven, S., Francus, P., Lamoureux, S.F., 2010. Estimation of grain size variability with micro X-ray fluorescence in laminated lacustrine sediments, Cape Bounty, Canadian High Arctic. J. Paleolimnol. 44, 803–817.
Dallmann, W.K., 2015. Geoscience atlas of Svalbard. Rapp. Nor. Polarinst. 148, 1–292.
Davies, S.J., Lamb, H.F., Roberts, S.J., 2015. Micro-XRF core scanning in palaeolimnology: recent developments. In: Croudace, I., Rothwell, R. (Eds.), Micro-XRF Studies of Sediment Cores. Developments in Paleoenvironmental Research, vol. 17. Springer, Dordrecht, pp. 189–226.
Eidesen, P.B., Carlsen, T., Molau, U., Brochmann, C., 2007. Repeatedly out of Beringia: Cassiope tetragona embraces the arctic. J. Biogeogr. 34, 1559–1574.
Eidesen, P.B., Strømmen, K., Vader, A., 2013. Fjelltettegras Pinguicula alpina funnet ny for Svalbard i Ringhorndalen. Blyttia 71, 209–213.
Eidesen, P.B., Arnesen, G., Elven, R., Søli, G., 2018. Kartlegging av Ringhorndalen, Wijdefjorden: en uutforsket arktisk oase, Report to the Governor of Svalbard. The University Centre in Svalbard, The University of Oslo, Ecofact Nord AS.
Elvebakk, A., 1989. Biogeographical Zones of Svalbard and Adjacent Areas Based on Botanical Criteria. Dr. scient. thesis. University of Tromsø, Norway.
Elvebakk, A., 1994. A survey of plant associations and alliances from Svalbard. J. Veg. Sci. 5, 791–802.
Elvebakk, A., 2005. 'Arctic hotspot complexes' – proposed priority sites for studying and monitoring effects of climatic change on arctic biodiversity. Phytocoenologia 35, 1067–1079. https://doi.org/10.1127/0340-269x/2005/0035-1067.
Elvebakk, A., Nilsen, L., 2002. Indre Wijdefjorden Med Sidefjordar: Eit Botanisk Unikt Steppeområde. Rapport Til Sysselmannen På Svalbard. University of Tromsø, Tromsø.
Elvebakk, A., Nilsen, L., 2016. Stepperøyrkvein Calamagrostis purpurascens i Wijdefjorden på Svalbard - einaste lokalitetar i Europa. Blyttia 74, 259–266.
Elven, R., Murray, D.F., Razzhivin, V., Yurtsev, B.A., 2011. Checklist of the Panarctic Flora (PAF). Natural History Museum, University of Oslo, Oslo. www.panarcticflora.org. (Accessed 24 October 2018).
Engelskjøn, T., Lund, L., Alsos, I.G., 2003. Twenty of the most thermophilous vascular plant species in Svalbard and their conservation state. Polar Res. 22, 317–339.
Farnsworth, W.R., 2018. Holocene Glacier History of Svalbard: Retracing the Style of (De-)glaciation. Doctoral thesis. UiT The Arctic University of Norway, Tromsø, ISBN 978-82-8236-325-9, p. 226. https://munin.uit.no/handle/10037/14378.
Farnsworth, W.R., Ingólfsson, Ó., Retelle, M., Allaart, L., Håkansson, L., Schomacker, A., 2018. Svalbard glaciers re-advanced during the Pleistocene-Holocene transition. Boreas 47, 1022–1032.
Ficetola, G.F., Pansu, J., Bonin, A., Coissac, E., Giguet-Covex, C., De Barba, M., Gielly, L., Lopes, C.M., Boyer, F., Pompanon, F., 2015. Replication levels, false presences and the estimation of the presence/absence from eDNA metabarcoding data. Mol. Ecol. Resour. 15, 543–556.
Forman, S., Lubinski, D., Ingólfsson, Ó., Zeeberg, J., Snyder, J., Siegert, M., Matishov, G., 2004. A review of postglacial emergence on Svalbard, Franz Josef land and Novaya Zemlya, northern Eurasia. Quat. Sci. Rev. 23, 1391–1434.
Gjerde, M., Bakke, J., D'Andrea, W.J., Balascio, N.L., Bradley, R.S., Vasskog, K., Ólafsdóttir, S., Røthe, T.O., Perren, B.B., Hormes, A., 2017. Holocene multi-proxy environmental reconstruction from lake Hakluytvatnet, Amsterdamøya island, Svalbard (79.5°N). Quat. Sci. Rev. 183, 164–176. https://doi.org/10.1016/j.quascirev.2017.02.017.
Göttlich, K., Hornburg, P., 1982. Ein Zeuge warmezeitlicher Moore im Adventdalen auf Spitsbergen (Svalbard-Archipel. Telma 12, 253–260.
Grimm, E.C., 1987. CONISS: a FORTRAN 77 program for stratigraphically constrained cluster analysis by the method of incremental sum of squares. Comput. Geosci. 13, 13–35.
Guiry, M.D., Guiry, G.M., 2018. AlgaeBase. World-wide Electronic Publication. National University of Ireland, Galway. http://www.algaebase.org. (Accessed 24 October 2018).
Hagen, J.O., Liestøl, O., Roland, E., Jørgensen, T., 1993. Glacier Atlas of Svalbard and Jan Mayen, vol. 129. Norwegian Polar Institute Meddelelser.
Hald, M., Ebbesen, H., Forwick, M., Godtliebsen, F., Khomenko, L., Korsun, S., Ringstad Olsen, L., Vorren, T.O., 2004. Holocene paleoceanography and glacial history of the West Spitsbergen area, Euro-Arctic margin. Quat. Sci. Rev. 23, 2075–2088.
Heiri, O., Lotter, A.F., Lemcke, G., 2001. Loss on ignition as a method for estimating organic and carbonate content in sediments: reproducibility and comparability of results. J. Paleolimnol. 25, 101–110.
Hofreiter, M., Serre, D., Poinar, H., Kuch, M., Pääbo, S., 2001. Ancient DNA. Nat. Rev. Genet. 2, 353–359. https://doi.org/10.1038/35072071.
Hormes, A., Gjermundsen, E.F., Rasmussen, T.L., 2013. From mountain top to the deep sea – deglaciation in 4D of the northwestern Barents Sea ice sheet. Quat. Sci. Rev. 75, 78–99.
Hyvärinen, H., 1968. Late-Quaternary sediment cores from lakes on Bjørnøya. Geogr. Ann. 50 A, 235–245.
Hyvärinen, H., 1969. Trullvatnet: a Flandrian stratigraphical site near Murchisonfjorden, Nordaustlandet, Spitsbergen. Geogr. Ann. 51 A, 42–45.
Hyvärinen, H., 1970. Flandrian pollen diagrams from Svalbard. Geogr. Ann. 52 A, 213–222.
Jónsdóttir, I.S., 2005. Terrestrial ecosystems on Svalbard: heterogeneity, complexity and fragility from an arctic island perspective. In: Biology and Environment: Proceedings of the Royal Irish Academy, 105B, pp. 155–165.
Juggins, S., 2017. Rioja: Analysis of Quaternary Science Data, R Package Version (0.9-15.1). http://cran.r-project.org/package=rioja.
van der Knaap, W.O., 1989. Past vegetation and reindeer on Edgeøya (Spitsbergen) between c. 7900 and c. 3800 BP, studied by means of peat layers and reindeer faecal pellets. J. Biogeogr. 16, 379–394.
Kylander, M.E., Ampel, L., Wohlfarth, B., Veres, D., 2011. High-resolution X-ray fluorescence core scanning analysis of Les Echets (France) sedimentary sequence: new insights from chemical proxies. J. Quat. Sci. 26, 109–117. https://doi.org/10.1002/jqs.1438.
Lamb, H.F., Edwards, M.E., 1988. The Arctic, Vegetation History. Springer, pp. 519–555.
Larsen, E.A., Lyså, A., Rubensdotter, L., Farnsworth, W.R., Jensen, M., Nadeau, M.J., Ottesen, D., 2018. Late-glacial and Holocene glacier activity in the van Mijenfjorden area, western Svalbard. arktos 4, 1–9. https://doi.org/10.1007/s41063-018-0042-2.
Liu, X., Colman, S.M., Brown, E.T., Minor, E.C., Li, H., 2013. Estimation of carbonate, total organic carbon, and biogenic silica content by FTIR and XRF techniques in lacustrine sediments. J. Paleolimnol. 50, 387–398.
Löwemark, L., Chen, H.F., Yang, T.N., Kylander, M., Yu, E.F., Hsu, Y.W., Lee, T.Q., Song, S.R., Jarvis, S., 2011. Normalizing XRF-scanner data: a cautionary note on the interpretation of high-resolution records from organic-rich lakes. J. Asian Earth Sci. 40, 1250–1256. https://doi.org/10.1016/j.jseaes.2010.06.002.
Luoto, T.P., Ojala, A.E.K., Arppe, L., Brooks, S.J., Kurki, E., Oksman, M., Wooller, M.J., Zajączkowski, M., 2017. Synchronized proxy-based temperature reconstructions reveal mid- to late Holocene climate oscillations in High Arctic Svalbard. J. Quat. Sci. 33, 93–99. https://doi.org/10.1002/jqs.3001.
Mangerud, J., Svendsen, J.I., 2018. The Holocene thermal maximum around Svalbard, arctic North Atlantic; molluscs show early and exceptional warmth. Holocene 28, 65–83. https://doi.org/10.1177/0959683617715701.
Melles, M., Brigham-Grette, J., Minyuk, P.S., Nowaczyk, N.R., Wennrich, V., DeConto, R.M., Anderson, P.M., Andreev, A.A., Coletti, A., Cook, T.L., 2012. 2.8 million years of Arctic climate change from Lake El'gygytgyn, NE Russia. Science

337 (6092), 315–320. https://doi.org/10.1126/science.1222135.
Miller, G.H., Brigham-Grette, J., Alley, R.B., Anderson, L., Bauch, H.A., Douglas, M.S.V., Edwards, M.E., Elias, S.A., Finney, B.P., Fitzpatrick, J.J., Funder, S.V., Herbert, T.D., Hinzman, L.D., Kaufman, D.S., MacDonald, G.M., Polyak, L., Robock, A., Serreze, M.C., Smol, J.P., Spielhagen, R., White, J.W.C., Wolfe, A.P., Wolff, E.W., 2010. Temperature and precipitation history of the Arctic. Quat. Sci. Rev. 29, 1679–1715. https://doi.org/10.1016/j.quascirev.2010.03.001.
Miller, G.H., Landvik, J.Y., Lehman, S.J., Southon, J.R., 2017. Episodic Neoglacial snowline descent and glacier expansion on Svalbard reconstructed from the 14C ages of ice-entombed plants. Quat. Sci. Rev. 155, 67–78.
Missouri Botanical Garden, 2018. Tropicos.org. http://www.tropicos.org.
Müller, J., Werner, K., Stein, R., Fahl, K., Moros, M., Jansen, E., 2012. Holocene cooling culminates in sea ice oscillations in Fram Strait. Quat. Sci. Rev. 47, 1–14.
Myers, N., Mittermeier, R.A., Mittermeier, C.G., da Fonseca, G.A.B., Kent, J., 2000. Biodiversity hotspots for conservation priorities. Nature 403, 853–858. https://doi.org/10.1038/35002501.
Oksanen, J., Blanchet, F.G., Friendly, M., Kindt, R., Legendre, P., McGlinn, D., Minchin, P.R., O'hara, R.B., Simpson, G.L., Solymos, P., Stevens, M.H.H., Szoecs, E., Wagner, H., 2017. Vegan: Community Ecology Package. R Package version 2.4-4. https://CRAN.R-project.org/package=vegan.
Pansu, J., Giguet-Covex, C., Ficetola, G.F., Gielly, L., Boyer, F., Zinger, L., Arnaud, F., Poulenard, J., Taberlet, P., Choler, P., et al., 2015. Reconstructing long-term human impacts on plant communities: an ecological approach based on lake sediment DNA. Mol. Ecol. 24 (7), 1485–1498. https://doi.org/10.1111/mec.13136.
Parducci, L., Bennett, K.D., Ficetola, G.F., Alsos, I.G., Suyama, Y., Wood, J.R., Pedersen, M.W., 2017. Ancient plant DNA from lake sediments: notes S1 Bioinformatic tools for metabarcoding datasets. New Phytol. 214, 924–942. https://doi.org/10.1111/nph.14470.
Pedersen, M.W., Ruter, A., Schweger, C., Friebe, H., Staff, R.A., Kjeldsen, K.K., Mendoza, M.L., Beaudoin, A.B., Zutter, C., Larsen, N.K., Potter, B.A., Nielsen, R., Rainville, R.A., Orlando, L., Meltzer, D.J., Kjær, K.H., Willerslev, E., 2016. Postglacial viability and colonization in North America's ice-free corridor. Nature 537, 45–49. https://doi.org/10.1038/nature19085.
R Core Team, 2017. R: A Language and Environment for Statistical Computing (Computer Program). R Foundation for Statistical Computing, Vienna. Available at: https://www.R-project.org/.
Reimer, P.J., Bard, E., Bayliss, A., Beck, J.W., Blackwell, P.G., Ramsey, C.B., Buck, C.E., Cheng, H., Edwards, R.L., Friedrich, M., et al., 2013. Intcal13 and Marine13 radiocarbon age calibration curves 0-50,000 Years cal bp. Radiocarbon 55, 1869–1887. https://doi.org/10.2458/azu_js_rc.55.16947.
Røthe, T.O., Bakke, J., Vasskog, K., Gjerde, M., D'Andrea, W.J., Bradley, R.S., 2015. Arctic Holocene glacier fluctuations reconstructed from lake sediments at Mitrahalvøya, Spitsbergen. Quat. Sci. Rev. 109, 111–125. https://doi.org/10.1016/j.quascirev.2014.11.017.
Røthe, T.O., Bakke, J., Støren, E.W.N., Bradley, R.S., 2018. Reconstructing Holocene glacier and climate fluctuations from lake sediments in Vårfluesjøen, northern Spitsbergen. Front. Earth Sci. 6, 1–20.
Rothwell, R.G., Croudace, I.W., 2015. Twenty years of XRF core scanning marine sediments: what do geochemical proxies tell us?. In: Developments in Paleoenvironmental Research, Micro-XRF Studies of Sediment Cores, pp. 25–102.
Rothwell, R.G., Rack, F.R., 2006. New Techniques in Sediment Core Analysis: an Introduction. Special Publications, vol. 267. Geological Society, London.
Rothwell, G., Hoogakker, B., Thompson, J., Croudace, I.W., Frenz, M., 2006. Turbidity emplacement on the southern Balearic Abyssal Plain (western Mediteranean Sea) during Marine Isotope Stages 1-3: an application of ITRAX XRF scanning of sediment cores to litostratigraphic analysis. In: Rothwell, R.G. (Ed.), New Techniques in Sediment Core Analysis, vol. 267. Special Publications, London, pp. 79–98. Geological Society.
Salvigsen, O., Høgvard, K., 2006. Glacial history, Holocene shoreline displacement and palaeoclimate based on radiocarbon ages in the area of Bockfjorden, northwestern Spitsbergen, Svalbard. Polar Res. 25, 15–24.
Sandgren, P., Snowball, I., 2001. Application of mineral magnetic techniques to paleolimnology. In: Last, W.M., Smol, J.P. (Eds.), Vol. 2 *Tracking Environmental Change Using Lake Sediments, Physical and Chemical Techniques*. Kluwer Academic Publishers, Dordrecht, The Netherlands.
Schomacker, A., Farnsworth, W.R., Ingólfsson, Ó., Allaart, L., Håkansson, L., Retelle, M., Siggaard-Andersen, M.-L., Korsgaard, N.J., Rouillard, A., Kjellman, S.E., 2019. Postglacial relative sea level change and glacier activity in the early and late Holocene: Wahlenbergfjorden, Nordaustlandet, Svalbard. Sci. Rep. 9, 6799. https://doi.org/10.1038/s41598-019-43342-z.
Snowball, I., Sandgren, P., 1996. Lake sediment studies of Holocene glacial activity in the Kårsa valley, northern Sweden: contrasts in interpretation. Holocene 6, 367–372.
Soininen, E.M., Gauthier, G., Bilodeau, F., Berteaux, D., Gielly, L., Taberlet, P., Gussarova, G., Bellemain, E., Hassel, K., Stenoien, H.K., et al., 2015. Highly overlapping winter diet in two sympatric lemming species revealed by DNA metabarcoding. PloS One 10, e0115335. https://doi.org/10.1371/journal.pone.0115335.
Sønstebø, J.H., Gielly, L., Brysting, A.K., Elven, R., Edwards, M., Haile, J., Willerslev, E., Coissac, E., Rioux, D., Sannier, J., Taberlet, P., Brochmann, C., 2010. Using next-generation sequencing for molecular reconstruction of past Arctic vegetation and climate. Mol. Ecol. Resour. 10, 1009–1018. https://doi.org/10.1111/j.1755-0998.2010.02855.x.
Taberlet, P., Coissac, E., Pompanon, F., Gielly, L., Miquel, C., Valentini, A., Vermat, T., Corthier, G., Brochmann, C., Willerslev, E., 2007. Power and limitations of the chloroplast trnL (UAA) intron for plant DNA barcoding. Nucleic Acids Res. 35, e14. https://doi.org/10.1093/nar/gkl938.
Taberlet, P., Bonin, A., Coissac, E., Zinger, L., 2018. Environmental DNA: for Biodiversity Research and Monitoring. Oxford University Press.
Thompson, R., Battarbee, R.W., Osullivan, P.E., Oldfield, F., 1975. Magnetic-susceptibility of lake sediments. Limnol. Oceanogr. 20, 687–698. https://doi.org/10.4319/lo.1975.20.5.0687.
Torti, A., Lever, M.A., Jørgensen, B.B., 2015. Origin, dynamics, and implications of extracellular DNA pools in marine sediments. Mar. Genom. 24, 185–196. https://doi.org/10.1016/j.margen.2015.08.007.
Vasil'chuk, A., 2005. Taphonomic features of Arctic pollen. Biol. Bull. 32, 196–206.
Wagner, B., Bennike, O., Cremer, H., Klug, M., 2010. Late quaternary history of the Kap Mackenzie area, northeast Greenland. Boreas 39, 492–504. https://doi.org/10.1111/j.1502-3885.2010.00148.x.
de Wet, G.A., Balascio, N.L., D'Andrea, W.J., Bakke, J., Bradley, R.S., Perren, B., 2018. Holocene glacier activity reconstructed from proglacial lake Gjøavatnet on Amsterdamøya, NW Svalbard. Quat. Sci. Rev. 183, 188–203. https://doi.org/10.1016/j.quascirev.2017.03.018.
Willerslev, E., Davison, J., Moora, M., Zobel, M., Coissac, E., Edwards, M.E., Lorenzen, E.D., Vestergard, M., Gussarova, G., Haile, J., et al., 2014. Fifty thousand years of Arctic vegetation and megafaunal diet. Nature 506 (7486), 47–51. https://doi.org/10.1038/nature12921.
Willis, K.J., Araújo, M.B., Bennett, K.D., Figueroa-Rangel, B., Froyd, C.A., Myers, N., 2007. How can a knowledge of the past help to conserve the future? Biodiversity conservation and the relevance of long-term ecological studies. Phil. Trans. Biol. Sci. 362 (1478), 175–187.
Wohlfarth, B., Lemdahl, G., Olsson, S., Persson, T., Snowball, I., Ising, J., Jones, V., 1995. Early Holocene environment on Bjørnøya (Svalbard) inferred from multidisciplinary lake sediments studies. Polar Res. 14, 253–275. https://doi.org/10.3402/polar.v14i2.6667.
Zimmermann, H.H., Raschke, E., Epp, L.S., Stoof-Leichsenring, K.R., Schirrmeister, G., Schwamborn, L., Herzschuh, U., 2017a. The history of tree and shrub taxa on Bol'shoy Lyakhovsky Island (New Siberian Archipelago) since the Last Interglacial uncovered by sedimentary ancient DNA and pollen data. Genes 8, 273. https://doi.org/10.3390/genes8100273.
Zimmermann, H.H., Raschke, E., Epp, L.S., Stoof-Leichsenring, K.R., Schirrmeister, G., Schwamborn, L., Herzschuh, U., 2017b. Sedimentary ancient DNA and pollen reveal the composition of plant organic matter in Late Quaternary permafrost sediments of the Buor Khaya Peninsula (north-eastern Siberia). Biogeosciences 14, 575–596. https://doi.org/10.5194/bg-14-575-2017.